Applied Energy 381 (2025) 125103

Contents lists available at ScienceDirect

Applied Energy

journal homepage: www.elsevier.com/locate/apenergy

Optimizing trading of electric vehicle charging flexibility in the continuous intraday market under user and market uncertainties

Raviteja Chemudupaty *, Timothée Hornek *, Ivan Pavić, Sergio Potenciano Menci

Interdisciplinary Centre for Security, Reliability and Trust - SnT, University of Luxembourg, 29 Avenue John F. Kennedy, Kirchberg Luxembourg, 1855, Luxembourg

GRAPHICAL ABSTRACT

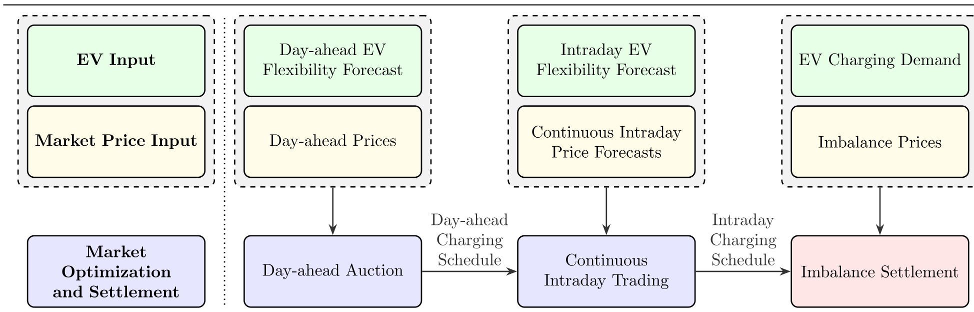

ARTICLE INFO

Keywords:
Electric vehicle flexibility
Multi-stage optimization
Continuous intraday market
Electric vehicle user uncertainty
Short-term electricity price forecasting

ABSTRACT

The rise in electric vehicles (EVs) challenges energy suppliers with unpredictable charging behavior, making demand forecasts less accurate and increasing financial risks from power imbalances. In Europe, retailers can trade these imbalances in short-term markets like the continuous intraday (CID) market. By controlling EV charging times, suppliers can shift charging to periods with lower prices, potentially benefiting financially. However, the financial gains from trading this flexibility in the CID market remain uncertain due to EV user behavior and price fluctuations. In this study, we develop and test trading strategies designed to manage the power needs of a fleet of 1000 EVs across different segments of short-term electricity markets, focusing on the day-ahead (DA) auction, and the CID market. To address EV-use uncertainty, we take an initial EV charging flexibility forecast for the DA auction, and an updated forecast for the CID market. We find that trading in the CID market reduces the overall cost of making power purchases by capitalizing on the flexibilities of EV charging times. Our results suggest that energy suppliers trading in the CID market significantly reduce their financial risk, even when there are high margins of error in EV flexibility forecasts. In our scenario with the highest deviation between the DA and intraday (ID) flexibility metrics, applying the best CID strategies yielded an average yearly profit of €37.52 and €4,840.63 in 2019 and 2022 respectively. In comparison to the baseline strategy, which clears volumes as imbalances, the corresponding financial savings amounted to €1978.52 and €16,632.25, respectively.

1. Introduction

There has been significant growth in the use of EVs in recent years, boosted by regulation and the provision of state-financed incentives. As this growth is expected to continue in the coming years [1], energy suppliers will need to meet growing power demands for EV charging [2].

Energy suppliers use EV demand forecasts to help them plan, with these often based on historical driving and charging patterns [3].

* Corresponding author.
E-mail addresses: raviteja.chemudupaty@uni.lu (R. Chemudupaty), timothee.hornek@uni.lu (T. Hornek).

https://doi.org/10.1016/j.apenergy.2024.125103
Received 5 April 2024; Received in revised form 11 November 2024; Accepted 3 December 2024
Available online 24 December 2024

However, due to the variable nature of EV users' driving behaviors and their evolving charging preferences, discrepancies arise between forecast and actual charging demand [4]. These discrepancies might pose financial risks for energy suppliers, particularly in European markets where market participants pay penalties if there are "imbalances" between expected and actual demand [5].

Energy suppliers in Europe can mitigate power imbalance penalties by participating in short-term electricity markets, such as the DA market and the CID market. In Europe, the main difference between these markets is their gate closure times. In the DA market, gate closure is typically around noon on the day prior to the product's due delivery date. In the CID market, trading occurs up to a few minutes before delivery, thus enabling energy suppliers to adjust schedules to real-time demand [5]. Furthermore, when charging EVs in a controlled manner (i.e. using "smart charging" techniques), EVs can serve as a flexible asset [6,7]. Energy suppliers can leverage the flexibility provided by EVs to charge the vehicles when prices are lower, enabling the energy supplier to reduce procurement costs [8,9]. However, there remains a lack of clarity regarding the potential financial gains and risks for energy suppliers regarding the trading of EV charging flexibility in the CID market. This is due to uncertainties in EV usage and electricity market price fluctuations.

In the interests of facilitating EV flexibility trading in the CID market, rolling window (RW) horizon optimization methods have been proposed [10,11]. RW horizon optimization models allow energy suppliers to adapt dynamically to CID market conditions. By using a sequential trading strategy, energy suppliers can first acquire most of the power required to satisfy charging needs from the DA market while minimizing costs, and then also realize arbitrage gains by trading on the CID market [11,12]. Modeling price uncertainties in the CID market is achieved by modeling different price scenarios with their associated probabilities [12,13]. When modeling EVs flexibility, many authors [11,12,14] assumed that the forecast demand from EVs would remain constant when trading in the DA and CID markets.

Relying solely on the same DA EV demand forecasts when trading in the CID market could be impractical. DA demand forecasts (including EV power requirements) are typically generated at least 36 h before delivery, hence increasing the likelihood of inaccuracies due to changed circumstances. The closer a forecast is made to delivery time, the more accurate it will be thanks to the integration of the latest user data, such as on-going plug-in and plug-out times. Also, using the same forecast for both DA and CID markets risks overlooking potential additional imbalance costs stemming from changes in demand for EV charging capacity. Furthermore, including price uncertainty in modeled scenarios requires prior knowledge of market prices, as these scenarios often fit the whole modeling interval [12]. However, future market prices are difficult to predict, leading to unrealistic forecast scenarios which are poorly suited for practical applications. These require dynamic adaptation to changes in market prices. In our paper, we propose a novel optimization model that takes account of the uncertainties arising from (1) EV charging flexibility, and (2) price volatility in the CID market.

To effectively model the uncertainties implicit in the provision of EV charging flexibility, we quantify the flexibility of an EV fleet by stochastically combining individual flexibility metrics derived from a synthetic mobility dataset [15]. In our paper, we focus solely on the demands of EV charging at home, specifically unidirectional charging. Accordingly, we calculate the flexibility metrics for EVs connected to home charging stations. These flexibility metrics include measurements of power and energy over time. These metrics provide insights into the extent to which charging power can be adjusted at each time step of the process, while still ensuring that the EV battery receives sufficient charge to meet the user's needs when they are ready to depart. We generate two sets of flexibility metrics: one that serves as a forecast for the DA period, and a subsequent ID set updates the former, which then serves as a forecast for all ID trading activities.

To realistically capture price uncertainty in the CID market, we create a price forecasting model that features the average of the four most recent transactions in the current product. We thereby incorporate the latest market price information into the model [16]. This approach allows for optimized decisions to be made, given the difficulty of anticipating future CID market price movements. In contrast, we use realized market price data to evaluate the results of the optimization process, thus measuring performance against real-world conditions.

Consequently, in this paper, we examine three different trading strategies. In all three strategies, we first seek to procure most of the power needs required for EV charging from the DA market using the DA EV flexibility forecast. This is done while also seeking to minimize costs. During the subsequent ID period, market positions must be updated to account for the updated ID EV flexibility forecast. The three strategies feature different approaches to rescheduling during the ID period:

1. **Baseline Strategy**: This strategy settles power volumes necessary to fulfill the ID schedule for the imbalance price, known as "regelzonen bergreifender einheitlicher Bilanzausgleichsenergiepreis" (cross-control area uniform balancing energy price) (reBAP) in Germany [17]. The strategy minimizes the difference between DA and ID power needs, thereby reducing imbalances and the associated costs.
2. **Static CID Strategy**: Similar to the *baseline strategy*, this approach makes the same power volume adjustments but settles them in the CID market instead of treating them as imbalances. For simplicity, the strategy uses the ID_1, a price index published by the European Power Exchange (EPEX), which reflects the price during the final trading hour of each product in the CID market [18].
3. **Dynamic CID Strategy**: This strategy continuously adjusts positions in the CID market using a RW approach. The RW method allows multiple re-optimizations during the CID trading window, leveraging EV charging flexibility to arbitrage from changing prices between products trading in parallel.

We evaluate all strategies on German EPEX market data for two separate years, 2019 and 2022, thereby providing an understanding of the strategies' efficacy in different market conditions. Specifically, we quantify the benefit of adjusting positions taken in the DA market by trading in the CID market, as opposed to settling deviations as imbalances [5].

The remainder of the paper is structured as follows. Section 2 contains an introduction to the European wholesale power markets, particularly to CID markets, using Germany as an example. Furthermore, we discuss the literature on EV power flexibility modeling and trading. Section 3 introduces our sequential optimization model and CID trading strategies. Section 4 gives an overview of the data used in our paper. Section 5 covers the scenarios used for our simulations. Section 6 presents and discusses our simulation results. Section 7 concludes the paper.

2. Background and related work

Section 2.1 provides a brief overview of European electricity markets to facilitate understanding of the rest of the paper. Subsequently, Section 2.2 reviews related work and situates our study within the existing literature.

2.1. Background: Electricity spot markets

In Europe, power market participants such as energy suppliers can trade in short-term markets to reduce their demand and supply imbalances until just a few minutes before delivery. Although these markets are technically futures markets that feature a lag between trading and physical delivery, they are commonly referred to as spot markets [5]. Germany serves as an instructive case, as it is one of Europe's largest power markets by traded volume [19]. The German spot market includes a DA auction and an ID market. The ID market is divided into two parts: an auction market, known as the intraday auction (IDA) market, and a continuous market, referred to as the CID market. Products traded in the spot market are characterized by their different delivery time intervals, which can be one hour, thirty minutes, or fifteen minutes in length [20]. Within the German market, hourly products exhibit the highest liquidity, followed by quarter-hourly products [19,21]. Market participants such as energy suppliers can meet their short-term power needs by participating in the different parts of the spot market.

To participate in the European DA market, participants submit hourly orders to the DA auction, which clears through an auction mechanism. Orders can contain two types of offers: (1) bids, i.e., prices participants are willing to pay to buy power, and (2) asks, i.e., prices they are willing to accept to sell power. In Germany the DA auction takes place every day at noon for all hours of the following day [22]. Upon reaching the gate closure time (after which no more offers can be posted), a clearing algorithm matches these orders to establish a single product-specific clearing price for each market area, such as the German-Luxembourgish market area, adhering to the merit order principle [23].

While it is only possible to trade hourly products in the European DA market, the European ID market also allows trading in thirty minute and fifteen minute products [24]. The IDA works similarly to the DA auction and takes place every day at 3 PM for the products with delivery during the following day [22]. Unlike auctions, where all orders are cleared simultaneously based on the merit order principle, continuous trading in the CID market enables bids to be cleared continuously throughout the trading period. At 3 PM, trading in the European CID market starts [25]. In the CID market, the trading system instantaneously clears bids and asks whenever an ask price undercuts a bid [26]. In Germany, the CID market closes five minutes before delivery, i.e., before the start of the respective product.

After ID market closure ex-post imbalances are handled by transmission system operators (TSOs) [27]. All wholesale market participants belong to a balance responsible party (BRP), which compensates the TSOs for activating the balancing services required to minimize the imbalances caused by the activity of market players. It is important to note that the compensation can be negative, indicating a reversal in the direction of payment. In Germany, the compensation, (i.e., the imbalance price) is called the reBAP [17].

2.2. Related work: EV smart charging algorithms

Smart charging enables energy suppliers to manage EV charging, thereby reducing procurement costs by charging EVs when electricity prices are lower [28,29]. Properly estimating EV flexibility is crucial in developing smart charging algorithms. By accurately estimating the flexibility provided by EVs, energy suppliers could determine the potential for shifting the charging patterns while meeting EV users' energy requirements. This flexibility, derived from historical mobility patterns and charging preferences, requires accurate modeling of EV usage [3].

EV usage is subject to several uncertainties due to variable driving patterns and charging preferences. EV uncertainties could be related to the number of vehicles connected to charging points at any moment, the arrival and departure times of the vehicles, and the energy required for powering EVs [30,31]. To capture EV uncertainty, the likelihood of various parameters, such as trip distance, trip duration, trip start/end times, and others, are characterized by probability distribution functions (PDFs) [32].

These PDFs then serve as an input to Monte Carlo simulations, where stochastic EV usage patterns are modeled by drawing various EV parameters from the PDFs [33,34]. Another approach to model the stochastic EV usage patterns is by using a Markov chain. In a Markov chain, the transition between driving, parking/charging at different locations (e.g. workplace, home, commercial areas), and other states are determined by using transition probabilities [35,36]. The transition probabilities give the likelihood of the EV moving from one state to another in the next time step, with this based solely on the current state. These aid in developing a discrete-time state Markov chain which captures the spatio-temporal dynamics of EV usage over defined intervals (15 min, 30 min, 1 h) for a specific period (week, month, year) [15,37].

With these usage patterns as inputs, the charging demand is estimated by implementing an uncontrolled charging regime in which an EV is charged at full power until its requested energy need is fulfilled [38]. The energy required for a charging session is assumed to be equal to the estimated energy consumption of the EV for its next trip, or the energy required to reach maximum battery capacity. The necessary charging time can be calculated from the maximum charging power and the required energy. The load profile, which gives an electricity consumption pattern of each EV, is calculated and superimposed, representing the overall demand of EVs at each time step for a given time period [39,40].

To smart charge EVs, EV charging scheduling can be formulated as a mathematical optimization problem. This is because smart charging typically involves allocating resources (i.e., charging power) to maximize the objectives (such as minimizing energy supplier costs) while satisfying constraints (e.g. user requirements). In this notion, smart charging algorithms can employ stochastic optimization models to optimally schedule EV charging whilst dealing with uncertainties [41]. A stochastic optimization model utilizes probability distributions to represent uncertainties, allowing the model to account for a spectrum of potential scenarios [42]. When formulating objective functions to minimize costs for an energy supplier, various approaches are used. For instance, the objective function might focus on maximizing the expected profits in the DA market by calculating the average performance across different EV demand scenarios, based on their respective probabilities [43]. Additionally, some stochastic optimization models incorporate risk measures such as conditional value at risk (CVaR) [41,44,45] or variance [42] into the objective function, which could be to minimize the costs in the DA market [44] or maximize the energy suppliers profits [45]. Authors in [46] propose a hybrid stochastic and Information Gap Decision Theory (IGDT) optimization to maximize the EV aggregator profits. EV uncertainties are modeled with scenarios, while price risk is handled through IGDT.

Authors in [41,43,44,46] focused on the trading of EV flexibility primarily in DA markets. This is because these markets often exhibit more stable and predictable price patterns compared to ID markets, thus making it easier to model and optimize EV charging schedules.

However, by participating in DA and ID markets, energy suppliers can spread their risk exposure and hedge against the uncertainties created by fluctuating EV usage and market prices. Day-ahead markets offer energy suppliers foresight to help them plan strategically for the manifestation of anticipated patterns, while ID markets provide the flexibility to respond quickly to unforeseen changes in EV demand. The ID markets are also referred to as real-time (RT) markets in some electricity markets, such as the Iberian market [47], the Nordic RT market [48], and the PJM (US based) RT market [34,49].

Two-stage optimization models enable energy suppliers to optimize EV charging in both DA and RT/ID markets. The first-stage decisions usually correspond to DA market scheduling with the objective of minimizing the costs of the energy supplier. The second-stage decisions usually correspond to RT/ID markets where authors in [34,47] model the objective function in order to reduce the power imbalances and minimize the energy supplier's costs. Liu et al. [48] formulated the objective function to maximize the revenues of the energy supplier while considering bidirectional charging. Many authors [34,48,49] assumed perfect foresight, while in reality, market prices are uncertain and not known in advance, as explained in Section 2.1. To model the uncertainty in market prices, the authors in Sánchez-Martín et al. [47]

Table 1
Literature overview — Electricity markets
† non-German market.

Research paper	Electricity markets		
	DA	IDA	CID
Al-Awami and Sortomme [44]	✓	✗	✗
Aliasghari et al. [46]	✓	✗	✗
Balram et al. [45]	✓	✗	✗
Xu et al. [41]	✓	✗	✗
Zheng et al. [43]	✓	✗	✗
Liu et al. [48]	✓	✓†	✗
Jin et al. [34]	✓	✓†	✗
Silva et al. [49]	✓	✓†	✗
Sánchez-Martín et al. [47]	✓	✓†	✗
Naharudinsyah and Limmer [10]	✗	✗	✓
Chemudupaty et al. [51]	✓	✗	✓
Tepe et al. [11]	✓	✗	✓
Corinaldesi et al. [52]	✓	✗	✓
Shinde et al. [13]	✓	✗	✓
Vardanyan and Madsen [12]	✓	✓	✓
Meese et al. [50]	✓	✓	✓
Our paper	✓	✗	✓

employed forecasting models which predict price movements in ID markets. Meanwhile, the authors in [34,47–49] focused on modeling RT/ID markets which are similar to the IDA, where products are not traded continuously, as we explained in Section 2.1.

To capture the dynamics of the CID markets where trading occurs continuously, authors in [10,11] proposed an RW horizon optimization method to optimize the EV charging schedule. The RW method divides the problem into several windows over a specific time frame, allowing continuous adaptation of evolving constraints and data. Consequently, in the context of EV charging, the RW optimization model facilitates the recurrent updating of EV scheduling decisions within each window, while still minimizing the energy supplier's costs when trading in CID markets [10,13]. To represent the CID prices, authors implemented two approaches. In the first approach, authors in [11,50,51] consider single prices for each product. While in the second approach, authors in [10,14] consider multiple prices along the trading period. Multi-price modeling considers the price evolution within the trading sessions of CID products by reoptimizing positions repeatedly throughout the trading period [12,52]. At every repetition, the optimizations require price inputs to calculate the energy supplier's costs, since the optimization objectives rely on minimizing costs. Most authors [10,11,50, 52] assumed perfect foresight of CID prices. Other authors in [12,13, 51] model the prices by assuming different scenarios, with associated probabilities to account for uncertainty in CID prices.

In sequential trading across DA and ID markets, authors in [11,50] procured most of the power required for EV charging from the DA market while still minimizing costs. Subsequently, the authors in [11, 50] only traded power in the ID markets if this produces additional revenues. However, while modeling EV flexibility, most authors in [11–13,50–52] assumed the same EV demand forecast for both DA and ID markets. Thus, they also did not account for the potential imbalances and additional costs that could be incurred due to changes in EV demand while trading in CID markets.

To draw attention to the contributions of our paper, we summarize our literature review and compare existing literature with our paper in Tables 1 and 2.

In Table 1, we present the electricity markets considered by various papers for trading EV flexibility. Our paper focuses on trading EV flexibility in DA and CID markets. We do not investigate the IDA due to it having a similar clearing mechanism to the DA auction and lower liquidity in the German market compared to the DA auction [19].

In Table 2, we compile the papers that explore the trading of EV flexibility in CID markets, given our primary focus on modeling the CID market. We differentiate papers based on their approaches to CID price modeling and EV flexibility modeling. Table 2 lists all the papers focused on EV trading strategies within CID markets. We included all relevant studies from our initial search that addressed CID trading alongside EV flexibility. To the best of our knowledge, none of these papers integrated CID market price forecasts into their EV trading models. Our paper employs multiple prices for price modeling and utilizes price forecasts. By using price forecasts, we eliminate the need for prior knowledge of future prices during optimization. The price forecasting approach better reflects real-world trading scenarios, where decisions are made within trading sessions without prior knowledge of future price developments. We also consider the variation in EV demand between DA and CID markets. Therefore, we use an initial DA forecast for DA optimization, and update it with an ID forecast for CID trading. Using an updated ID forecast for CID trading enhances the accuracy of EV charging schedule optimization because the forecasts become more reliable over time. Additionally, we test different trading frequencies within the CID market and compare CID trading with settlement as an imbalance.

Table 2
Literature overview — CID Modeling.

Research paper	CID price modeling		Multistage EV modeling
	Multi-price	Price input	
Naharudinsyah and Limmer [10]	✓	perfect foresight	✗
Chemudupaty et al. [51]	✗	scenarios	✗
Tepe et al. [11]	✗	perfect foresight	✗
Corinaldesi et al. [52]	✓	perfect foresight	✗
Shinde et al. [13]	✓	scenarios	✗
Vardanyan and Madsen [12]	✓	scenarios	✗
Meese et al. [50]	✗	perfect foresight	✗
Our paper	✓	**price forecast**	✓

3. Methods

To enable the energy supplier to trade EV flexibility, we quantify the EV flexibility in terms of power and energy as functions of time. This will convey the information on the amount of power that can be varied in a controllable fashion during each time step, while maintaining the energy levels required to meet the users' requirements, and keeping charging power below charger limits. We then use this aggregated flexibility as an input to our optimization models to facilitate EV flexibility trading in both the DA and the CID markets. Fig. 1 illustrates the sequence of the different trading and optimization steps to obtain the final EV charging schedule.

Consistent with prevalent hedging strategies in short-term power markets, the objective is to meet all the power needs resulting from the DA EV flexibility forecast in the DA market while minimizing the procurement costs in line with [52]. Securing all volumes in the DA market is advantageous for hedging, offering higher liquidity than the CID [19] and a single clearing price per product. Conversely, continuous trading in the CID market increases risk due to fluctuating and volatile prices [53]. The model tries to find the cheapest periods in the DA timeframe to charge EVs without factoring in the ID markets or any possible imbalances. The DA optimization runs with the assumption of having perfect foresight of DA prices and an initial EV flexibility forecast, resulting in a preliminary DA charging schedule.

During the ID period, a more accurate EV flexibility forecast becomes available. For simplicity's sake, we assume that this forecast matches actual EV flexibility at the time of charging. To adjust the charging schedule to the updated flexibility forecast, we propose three strategies. The first strategy, the baseline strategy, aims to reschedule EV charging to minimize imbalances, specifically changes in the power of the EV charging schedule. Afterwards, the strategy settles remaining

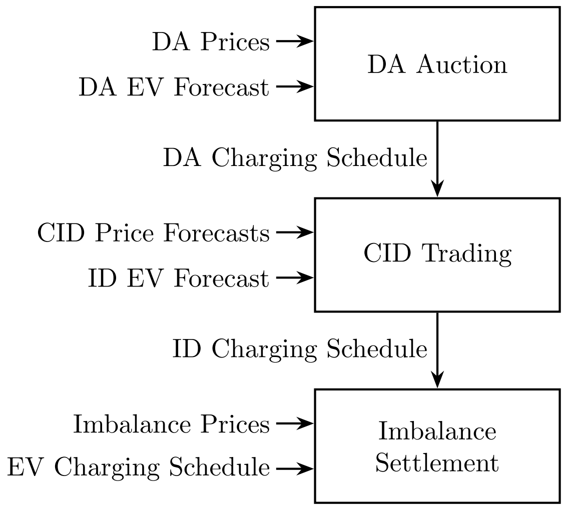

Fig. 1. Overview of trading steps.

imbalances for the reBAP. The second strategy, the static CID strategy, is similar, since it uses the same ID charging schedule. However, instead of settling power volumes for the reBAP, it settles power volumes in the CID market at the ID_1 price. The third strategy, the dynamic CID strategy, trades in the CID market, where the optimization model takes account of CID price forecasts. The strategy uses an RW approach, involving successive rounds of optimization and trading for the same product. Note, that opting to trade in the CID market eliminates imbalances, as all open volumes are traded in the CID market. All three strategies result in a final ID charging schedule, according to which EVs can be charged.

Section 3.1 quantifies the flexibility provided by an aggregated fleet of EVs. Sections 3.2 and 3.3 illustrate how our optimization models trade EV flexibility in the DA and CID markets, respectively. Section 3.4 summarizes the sequential optimization process.

3.1. EV flexibility model

3.1.1. Input parameters to quantify EV flexibility

In this Section, we outline the parameters of different user inputs, EV batteries, and EV chargers that are relevant for quantifying EV flexibility. The level of flexibility offered by an EV varies with each charging session; influenced by the user's driving and charging habits, as well as the EV battery and charger specification.

To quantify the EV flexibility, we need the maximum charging power of an EV charger, the plugin duration, and the energy that should be transferred within a charging session. The maximum charging power is the maximum power at which an EV can be charged ($P_v^{\max}$). The plugin duration is the time between EV arrival time (t^{arr}) and departure time (t^{dep}). The energy that should be transferred to satisfy the user's state of energy at departure ($\mathrm{SOE}^{\mathrm{dep}}$) requirement is denoted by E_v^{dep}.

In Fig. 2, we illustrate the typical EV battery with different energy values. $E_v^{\max}$ is the total battery capacity of the EV, E_v^{arr} is the EV battery capacity at the time of arrival (t^{arr}), and E_v^{dep} is the energy that should be transferred to satisfy the $\mathrm{SOE}^{\mathrm{dep}}$ requirement.

As we only consider unidirectional charging, the overall energy capacity of the battery can never drop below E_v^{arr}. Furthermore, the user might not always request maximum $\mathrm{SOE}^{\mathrm{dep}}$. This would mean that the sum of E_v^{arr} and E_v^{dep} would not always be equal to $E_v^{\max}$. Therefore, we only consider the part of the battery that can be charged i.e., E_v^{dep} while estimating EV flexibility.

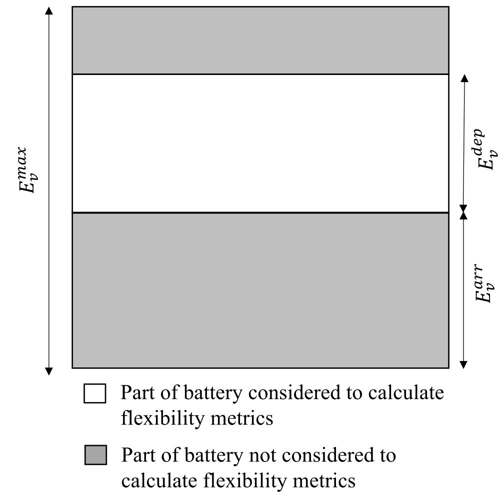

Fig. 2. Typical EV battery and different energy values.

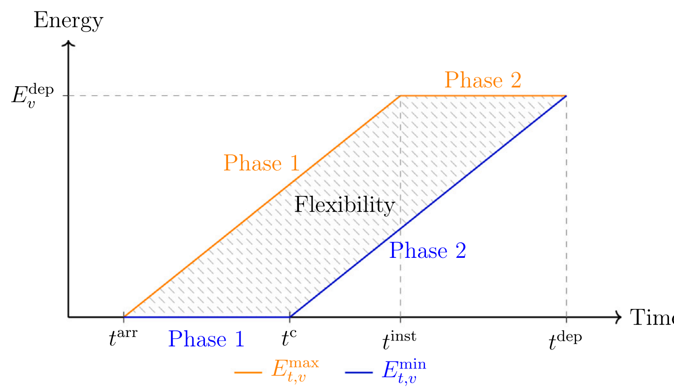

Fig. 3. Representation of EV flexibility in energy vs. time graph.

3.1.2. Quantification of individual EV flexibility

To estimate the flexibility provided by an EV, we quantify EV flexibility during its plugin duration using time-dependent energy and power metrics which are derived by using the parameters introduced in Section 3.1.1. The energy metrics are minimum energy ($E_{t,v}^{\min}$) and maximum energy ($E_{t,v}^{\max}$) at time t. The power metrics are minimum power ($P_{t,v}^{\min}$) and maximum power ($P_{t,v}^{\max}$) at time t. These metrics will convey the amount of power with which an EV can be charged while maintaining upper and lower limits of cumulative energy transfer.

$E_{t,v}^{\min}$ represents the minimum cumulative energy that must be transferred to the EV at time t to satisfy the user's energy requirement i.e., E_v^{dep}. The process to determine $E_{t,v}^{\min}$ is divided into two phases within its plugin duration as illustrated in Fig. 3.

The first phase is the idle state where there is no energy transfer to the EV until critical time (t^{c}). t^{c} marks the moment when the EV must begin charging at full power to meet the required energy level by departure time (E_v^{dep}). Therefore, the first phase to determine $E_{t,v}^{\min}$ extends from the t^{arr} to the t^{c}. The second phase covers the time between t^{c} and the time of departure (t^{dep}). During this phase, the EV is charged at full power to ensure that E_v^{dep} is achieved by the departure time. We present the mathematical formulation to determine $E_{t,v}^{\min}$ in Eqs. (1) and (2).

$$E_{t,v}^{\min} = E_{t-1,v}^{\min} + P_{t,v} \times \eta \times \Delta t \tag{1}$$

$$P_{t,v} = \begin{cases} 0 & t^{\mathrm{arr}} < t \leq t^{c} \quad \text{(Phase 1)} \\ P_v^{\max} & t^{c} < t \leq t^{\mathrm{dep}} \quad \text{(Phase 2)} \end{cases} \tag{2}$$

In reality, EV charging is not linear and involves different stages (such as constant current and constant voltage) to optimize the charging process for safety and battery health [54]. However, for simplicity, we assume linear charging of the EV where the charging power takes continuous values. Therefore, we calculate $E^{\min}_{t,v}$ by using Eq. (1), where $P_{t,v}$ is the charging power at time t, η is the charging efficiency to account for power losses while charging, and Δt is the time interval during which the charging power is delivered. The value of $P_{t,v}$ to calculate $E^{\min}_{t,v}$ in the first phase and the second phase are 0 and $P^{\max}_{v}$ respectively, as depicted in Eq. (2).

$E^{\max}_{t,v}$ represents the maximum cumulative energy that can be transferred to the EV at time t. Similar to $E^{\min}_{t,v}$, the process for determining $E^{\max}_{t,v}$ is divided into two distinct phases (as illustrated in Fig. 3).

In the first phase, the EV is charged instantaneously at maximum power until the energy required for departure, E^{dep}_{v}, is met. The duration of this phase is from t^{arr} (arrival time) to t^{inst}, where t^{inst} is the time needed to transfer E^{dep}_{v} instantaneously at full power. The second phase starts at t^{inst} and lasts until t^{dep} (departure time), during which no energy transfer occurs.

We present the mathematical formulation for calculating $E^{\max}_{t,v}$ in Eqs. (3) and (4). As we assume the linear charging of the EV, the maximum energy level at time t, $E^{\max}_{t,v}$ is calculated by Eq. (3). The $P_{t,v}$ value to calculate $E^{\max}_{t,v}$ in the first phase and second phase is $P^{\max}_{v}$ and 0 respectively, as depicted in Eq. (4).

$$E^{\max}_{t,v} = E^{\max}_{t-1,v} + P_{t,v} \times \eta \times \Delta t \tag{3}$$

$$P_{t,v} = \begin{cases} P^{\max}_{v} & t^{\mathrm{arr}} < t \leq t^{\mathrm{inst}} \quad \text{(Phase 1)} \\ 0 & t^{\mathrm{inst}} < t \leq t^{\mathrm{dep}} \quad \text{(Phase 2)} \end{cases} \tag{4}$$

When plotting $E^{\max}_{t,v}$ and $E^{\min}_{t,v}$ on the energy vs. time graph, the region bounded by these two energy metrics represents the degree of flexibility (see Fig. 3). As depicted in Fig. 3, the EV offers flexibility throughout the plugin duration, allowing the charging power to fluctuate between maximum and minimum possible values. This variation in charging power is possible as long as the cumulative energy transfer remains within the defined flexibility region. Therefore, the value of the minimum power flexibility metric - $P^{\min}_{t,v}$, which represents the minimum allowable power at which the EV must be charged at time t, is equal to 0 for the whole plugin duration.

The maximum power flexibility metric - $P^{\max}_{t,v}$, represents the maximum allowable power at which the EV can be charged at time t. Therefore, $P^{\max}_{t,v}$ for the whole plugin duration is equal to $P^{\max}_{v}$.

3.1.3. Quantification of EV fleet flexibility

As we manage a portfolio of an energy supplier, (which includes an EV fleet) aggregating their flexibilities becomes essential to facilitating trading in electricity markets. To obtain the aggregated flexibility of an EVs fleet, we sum up the flexibilities of individual EVs. We represent the resulting aggregated energy and power flexibility metrics as $E^{\min}_{t}$, $E^{\max}_{t}$ and $P^{\min}_{t}$, $P^{\max}_{t}$. These metrics characterize a virtual battery model, defined by its minimum and maximum thresholds for both power and energy levels. To account for uncertainties in EV flexibility forecasts, we generate different flexibility metrics for the DA and ID period by applying different weights to individual EV flexibility metrics during summation. Section 4.2 provides more details on the generation of the EV flexibility metrics. Consequently, we adapt the notation of the flexibility metrics to distinguish between both periods. Taking the minimum energy flexibility metric ($E^{\min}_{t}$) as an example, we denote the DA metric as $E^{\min,\mathrm{DA}}_{t}$ and the ID metric as $E^{\min,\mathrm{ID}}_{t}$.

3.2. DA optimization

We develop a linear optimization model with the objective of minimizing procurement costs incurred for charging the EV fleet. The input data for our optimization model are DA market prices and EV flexibility forecasts. The EV flexibility forecasts for the DA market are calculated using the flexibility model, detailed in Section 3.1. We assume perfect foresight of DA prices in line with [43]. This assumption allows us to isolate price uncertainty specifically within the CID market, aligning with our study's focus. Importantly, this assumption's impact is limited, as the DA schedule serves only as an initial reference for subsequent ID rescheduling, with our analysis centered on schedule changes made during the ID phase.

Our objective function aims to minimize the energy supplier's DA procurement costs (see Eq. (5)). The objective function considers the variable P^{DA}_{t} and parameter $C^{\mathrm{DA,true}}_{t}$, which are the power purchased from DA market and the DA price at time t, respectively. As we assume perfect foresight of the DA price, $C^{\mathrm{DA,true}}_{t}$ is the same as the clearing price of the DA market at time t.

$$\min_{P^{\mathrm{DA}}_{t}, E^{\mathrm{DA}}_{t}} \sum_{t} C^{\mathrm{DA,true}}_{t} \times P^{\mathrm{DA}}_{t} \times \Delta t \tag{5}$$

As we trade the aggregated flexibility of the EV fleet, we assume that all the EVs connected to their respective charging points at residential level create a large virtual battery [55]. In this regard, the power and energy flexibility metrics represent the minimum and maximum power and energy thresholds of the virtual battery (see Section 3.1.3). Therefore, $P^{\min,\mathrm{DA}}_{t}$ and $P^{\max,\mathrm{DA}}_{t}$ represent the minimum and maximum charging power of the virtual battery for the DA market at time t. While, $E^{\min,\mathrm{DA}}_{t}$ and $E^{\max,\mathrm{DA}}_{t}$ represent the minimum and maximum energy that could be transferred to the virtual battery at time t, for the DA market.

In the context of the virtual battery, P^{DA}_{t} represents the power procured from the DA market to charge the virtual battery. Thus, the P^{DA}_{t} value should always be between $P^{\min,\mathrm{DA}}_{t}$ and $P^{\max,\mathrm{DA}}_{t}$, ensured by the constraint formulated in Eq. (6):

$$P^{\min,\mathrm{DA}}_{t} \leq P^{\mathrm{DA}}_{t} \leq P^{\max,\mathrm{DA}}_{t} \quad \forall\, t \in T. \tag{6}$$

The variable E^{DA}_{t} represents the cumulative energy transferred to this virtual battery at time t in the DA market. The value of variable E^{DA}_{t} should always be within $E^{\min,\mathrm{DA}}_{t}$ and $E^{\max,\mathrm{DA}}_{t}$, ensured by the constraint formulated in Eq. (7):

$$0 \leq E^{\min,\mathrm{DA}}_{t} \leq E^{\mathrm{DA}}_{t} \leq E^{\max,\mathrm{DA}}_{t} \quad \forall\, t \in T. \tag{7}$$

The following Eq. (8) depicts the energy balance of the virtual battery:

$$E^{\mathrm{DA}}_{t} = E^{\mathrm{DA}}_{t-1} + P^{\mathrm{DA}}_{t} \times \Delta t - E^{\mathrm{left,DA}}_{t} \qquad \forall\, t \in T. \tag{8}$$

E^{DA}_{t} is the variable illustrating the cumulative energy transferred to the virtual battery at the time step t. Its value is affected by E^{DA}_{t-1}, P^{DA}_{t}, and $E^{\mathrm{left,DA}}_{t}$. E^{DA}_{t-1} is the cumulative energy transferred to the virtual battery in the previous time step. P^{DA}_{t} is the power procured to charge the virtual battery at the current time step t. $E^{\mathrm{left,DA}}_{t}$ is the cumulative energy transferred to the EVs that disconnect from the chargers at the current time step t, i.e., they no longer contribute to the virtual battery.

3.3. CID optimization

While we assume perfect foresight of DA market prices during DA optimization (see Section 3.2), we perform the CID optimization process using price forecasts of hourly CID products. Using price forecasts for CID optimization aligns with a realistic scenario in which trading decisions are made given uncertain knowledge of future prices. Given that the CID market is typically only highly liquid during the last few hours before delivery, we start optimization four hours before delivery [56].

Fig. 4 illustrates the simultaneous trading process for multiple hourly products, each represented by a distinct timeline. Each product is defined by two characteristics: the delivery start and the delivery period. The delivery start (indicated by the red dot) marks the exact

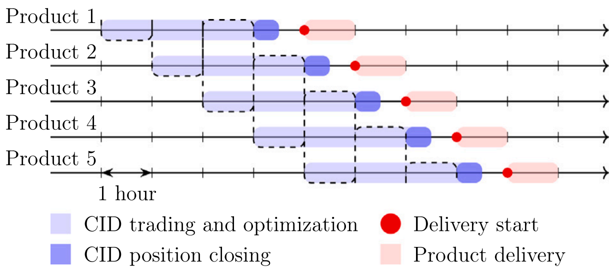

Fig. 4. Parallel trading of several hourly CID products.

moment when power delivery begins, while the delivery period (represented by the shaded area following the red dot) specifies the duration over which the power is supplied. For every product, the trading period opens four hours before delivery starts and closes half an hour before delivery starts. A timeline for a single product contains the following subintervals (from left to right): The chronological breakdown of a single product's timeline contains the following three segments:

1. The first segment spans three hours and covers the CID trading window of the respective product (light blue interval). This phase permits the re-optimization of the power schedule following updates in CID price forecasts.
2. The second segment, lasting 30 min, is a transition period where re-optimization ceases, yet the trading of remaining open positions continues (dark blue interval). Trading activity then stops 30 min before the start of delivery, which aligns with the decoupling of German control areas [25].
3. The third segment, which extends for one hour, denotes the product delivery period (light red interval). The start of this period is indicated by a red dot.

At any point in time, three hourly products can be traded in parallel, as highlighted by the dashed rectangles in Fig. 4.

We enter the CID market with an updated set of EV flexibility metrics, which may differ from the DA metrics (see Section 3.1.3). The updated flexibility metrics lead to updated ID constraints for the ID charging schedules depicted by the Eqs. (9), (10), and (11):

$$P_t^{\min,\mathrm{ID}} \leq P_t^{\mathrm{ID}} \leq P_t^{\max,\mathrm{ID}} \quad \forall t \in T, \tag{9}$$

$$0 \leq \; E_t^{\min,\mathrm{ID}} \leq \; E_t^{\mathrm{ID}} \leq \; E_t^{\max,\mathrm{ID}} \quad \forall t \in T, \tag{10}$$

$$E_t^{\mathrm{ID}} = E_{t-1}^{\mathrm{ID}} + P_t^{\mathrm{ID}} \times \Delta t - E_t^{\mathrm{left,ID}} \quad \forall t \in T. \tag{11}$$

The corresponding DA constraints are depicted by the Eqs. (6), (7), and (8). These constraint alterations could cause the DA solution (i.e., the planned EV charging schedule comprising E_t^{DA} and P_t^{DA}), to violate the new ID constraints. As a result, it becomes necessary to reoptimize the charging schedule to comply with the updated constraints, yielding an ID charging schedule comprising E_t^{ID} and P_t^{ID}.

We present three strategies for ID rescheduling. First, Section 3.3.1 discusses a baseline strategy aimed at minimizing deviations from the DA power schedule. The strategy settles power volumes as imbalances for the reBAP. Second, Section 3.3.2 introduces our static CID trading strategy, that relies on the market index ID_1 for power volume settlement. Third, Section 3.3.3 presents our dynamic CID trading strategy that takes advantage of parallel trading across different products. Parallel trading allows for arbitrage between the different CID products within the limits of the constraints for the ID schedule.

3.3.1. Baseline strategy

Our baseline strategy ignores market prices while rescheduling. Instead, it focuses solely on minimizing deviations from the DA schedule. Not considering market prices significantly reduces rescheduling complexity, since it allows for a single optimization run for every product. This method starkly contrasts with strategies aiming to capitalize on the CID market's continuous dynamics, which requires repeated optimization runs in a RW fashion (see Section 3.3.3). The baseline optimization serves as a benchmark for evaluating the continuous optimization strategy. The optimization approach is also valuable for market participants such as EV aggregators who aim to minimize imbalances without delving into the complexities of forecasting CID prices.

To express this strategy formally, for each product with a delivery start time of t, we reoptimize the power and energy schedules one hour before delivery, specifically at $t-1h$, using the objective function corresponding to Eq. (12):

$$\min_{P_k^{\mathrm{ID}},E_k^{\mathrm{ID}}} \sum_{k=t,t+1h,t+2h} |P_k^{\mathrm{DA}} - P_k^{\mathrm{ID}}|. \tag{12}$$

We apply the ID constraints given by the Eqs. (9), (10), and (11). The optimization aims to minimize the gap between the DA and ID EV power schedules, since any deviation requires market settlement. Although the formulation of the objective function (Eq. (12)) is non-linear, the objective function can be rendered linear (see Appendix A). Note that the optimization takes account of three products simultaneously. Also note that a single optimization iteration only fixes P_k^{ID} and E_k^{ID} for $k = t$, as the decision variables for products with a later delivery start (i.e., with larger k), might still undergo changes in subsequent rounds of optimization.

After calculating the new schedules, we contemplate two options for balancing the discrepancy between the DA power schedule P_t^{DA} and the ID power schedule P_t^{ID}. The first option involves settling open volumes as imbalances, effectively bypassing the CID market to settle the difference and invoice the imbalance price (reBAP). The corresponding formula for the ex-post evaluation of this approach is Eq. (13):

$$\sum_t C_t^{\mathrm{reBAP}} \times (P_t^{\mathrm{DA}} - P_t^{\mathrm{ID}}) \times \Delta t. \tag{13}$$

Settling for the imbalance price eliminates the need to trade in the CID market. This market can be complex due to its continuous nature.

3.3.2. Static CID strategy

Our second strategy reschedules power volumes in the same manner as the baseline strategy (see Section 3.3.1). However the strategy settles the power volumes financially in the CID market. According to the baseline optimization schedule, the final schedule for any product becomes known one hour before delivery, providing a half-hour trading window before the decoupling of the German control areas [25]. The ID_1 price index, a volume-weighted average published by the EPEX, reflects all transaction prices during this specific half-hour interval [18]. We employ the ID_1 price for settlement as it encompasses the relevant trading period. Moreover, the ID_1 serves as an indicator of the expected transaction price within the given interval — a price that can be expected in the long term. The corresponding formula for the ex-post evaluation is Eq. (14):

$$\sum_t C_t \times (P_t^{\mathrm{DA}} - P_t^{\mathrm{ID}}) \times \Delta t$$
$$-C^{\mathrm{CID,fee}} \times |P_t^{\mathrm{DA}} - P_t^{\mathrm{ID}}| \times \Delta t, \tag{14}$$

where $C^{\mathrm{CID,fee}}$ is a CID trading fee in €/MWh.

A limitation of this optimization strategy is that rescheduling is price agnostic, penalizing any deviation from the DA power schedule uniformly, regardless of variations in price signals. The subsequent section will present an approach that incorporates CID price dynamics and forecasts.

3.3.3. Dynamic CID strategy

This section explains our CID trading strategy, tailored to adapt to CID market trends. The foundation of our trading strategy lies in the DA schedule, available for all considered products during ID reoptimization. As Fig. 4 illustrates (see Section 3.3), at any time the CID strategy focuses on three hourly products at once in a RW fashion.

Limiting the optimization interval to a three-hour window, starting four hours before delivery, neglects charging needs beyond the three products considered in parallel at any time. In practice, this means that when prices are positive, the optimization may sell off any excess power not required within that window, neglecting future charging needs.

To address this issue, our CID optimization consists of two stages. The first stage identifies a "feasible energy target" based on the DA energy schedule. We use the DA schedule as a reference since it reflects power needs beyond the immediate CID optimization window, while still maintaining flexibility for trading within the current window. A "feasible energy target" is the minimum amount of energy that must be stored in the virtual battery at the defined product delivery time. Following this, the second stage trades in the CID market. The "feasible energy target" is the result of the first stage of our CID optimization.

The first stage runs two hours before the delivery start t of every product, i.e., at $t - 2h$. Eq. (15) depicts the objective function used to find a viable energy target for the product scheduled for delivery at $t + 2h$:

$$\min_{P_k^{\mathrm{ID,target}}, E_k^{\mathrm{ID,target}}} |E_{t+2h}^{\mathrm{DA}} - E_{t+2h}^{\mathrm{ID,target}}|, \tag{15}$$

where k represents the set of times $\{t, t+1h, t+2h\}$, covering the three hourly products that are traded simultaneously in the subsequent hour. Note, that the optimization adheres to the ID constraints (see Eqs. (9), (10), and (11)). The objective function (Eq. (15)) minimizes the difference between the scheduled DA and a feasible ID energy target ($E_{t+2h}^{\mathrm{ID,target}}$). When the DA schedule is feasible under the ID constraints, the energy target defaults to the DA schedule. The objective function (Eq. (15)) only considers the product with the latest delivery start ($t+2h$), as the goal is to align with the DA energy forecast in a longer-term perspective, thus providing flexibility in the preceding hours. The remaining flexibility can then be leveraged to trade in the CID market.

The second stage covers the CID trading approach. To model continuous trading, we introduce the additional index ℓ, representing continuous decision making during a specific hour. For every product with delivery start t, the optimization runs at $t - 2h + \frac{1h}{|L|} \times \ell$ for $\ell \in L$. For instance, when trading at quarter-hourly frequency, we obtain $L = \{0, 1, 2, 3\}$, given that $\frac{1h}{|L|} = 15min$. For every delivery start t and every index ℓ, we repeat the profit maximization optimization process with the objective function given by Eq. (16) to obtain the ID schedules for EV charging, which is composed of the power and energy schedules ($P_{k,\ell}^{\mathrm{ID}}$ and $E_{k,\ell}^{\mathrm{ID}}$ respectively):

$$\max_{P_{k,\ell}^{\mathrm{ID}}, E_{k,\ell}^{\mathrm{ID}}} \sum_{k=t,t+1h,t+2h} C_{k,\ell}^{\mathrm{CID,fcst}} \times (P_{k,\ell-1}^{\mathrm{ID}} - P_{k,\ell}^{\mathrm{ID}}) \times \Delta t$$
$$- C^{\mathrm{CID,fee}} \times |P_{k,\ell-1}^{\mathrm{ID}} - P_{k,\ell}^{\mathrm{ID}}| \times \Delta t. \tag{16}$$

This operates under the ID constraints (see Eqs. (9), (10), and (11)) and under the additional energy level constraint (Eq. (17)):

$$E_{t+2,\ell}^{\mathrm{ID}} \geq E_{t+2}^{\mathrm{ID,target}}. \tag{17}$$

This forces the energy schedule to meet or exceed the energy target $E_{t+2}^{\mathrm{ID,target}}$. The first term in the objective function estimates the value of trades which consider price forecasts $C_{k,\ell}^{\mathrm{CID,fcst}}$. Here, $P_{k,\ell-1}^{\mathrm{ID}} = P_t^{\mathrm{DA}}$ in the first iteration of ℓ. The second term considers volume-dependent trading fees $C^{\mathrm{CID,fee}}$.

From this optimization, we obtain $P_{k,\ell}^{\mathrm{ID}}$ and $E_{k,\ell}^{\mathrm{ID}}$ as the results, which enable the calculation of the trading profit for the current ℓ with the true future market prices $C_{k,\ell}^{\mathrm{CID,true}}$ using Eq. (18):

$$\sum_{k=t,t+1h,t+2h} C_{k,\ell}^{\mathrm{CID,true}} \times (P_{k,\ell-1}^{\mathrm{ID}} - P_{k,\ell}^{\mathrm{ID}}) \times \Delta t$$
$$- C^{\mathrm{CID,fee}} \times |P_{k,\ell-1}^{\mathrm{ID}} - P_{k,\ell}^{\mathrm{ID}}| \times \Delta t, \tag{18}$$

We repeat this procedure for all iterations of ℓ within a specific trading hour. Thus, the presented method aims to follow the DA energy schedule closely while executing a continuous optimization strategy in the CID market. This allows adaptation to ID constraints and offers a degree of freedom to facilitate a shift of power volumes between products.

Table 3
Overview of optimization processes.

DA	Stage 1	Objective	(5)	
		Constraints	(6), (7), (8)	
		Result	DA Schedule	
ID			Approach 1	Approach 2
	Stage 2	Objective	(12)	(15)
		Constraints	(9), (10), (11)	(9), (10), (11)
		Result	ID Schedule	Energy target
	Stage 3	Objective	N/A	(16)
		Constraints	N/A	(9), (10), (11), (17)
		Result	N/A	ID Schedule

3.4. Optimization process summary

To summarize the optimization processes discussed in this paper, Table 3 presents an overview. It lists the optimization stages along with references to the objective and constraints of the respective optimization problems. The first stage (Stage 1) contains the DA optimization procedure and yields a DA charging schedule. During the ID period, we propose two possible optimization approaches. First, the baseline strategy and the static CID strategy requires only one additional stage (Stage 2) to compute an ID charging schedule. Second, the dynamic CID strategy requires two additional optimization stages (Stage 2 and Stage 3). Stage 2 yields an energy target, i.e., a lower bound for the battery energy level. Afterwards, Stage 3 optimizes the CID schedule, taking into account the energy level bound from the previous stage. Regardless of the approach chosen, both approaches result in a final ID schedule for EV charging.

4. Data

The following section introduces the data we use in this paper. Section 4.1 outlines the mobility data. Section 4.2 describes the computation of flexibilities for both the DA and ID periods, based on the mobility data. Finally, Section 4.3 details the price data used in our study.

4.1. Mobility data

We use existing synthetic mobility data to derive the inputs required to calculate the flexibility metrics for each EV [15]. The synthetic mobility data stems from a German mobility survey [57]. The mobility data consists of 200 unique mobility profiles of residential EVs. The mobility profile is time series data that gives the location of the vehicle, the distance traveled, and the energy consumed every 15 min over a one year period. We analyze only the home charging case since majority of the vehicles currently charge at home [58], with the following assumptions:

- All vehicles charge at home as our focus is on home charging.
- To simplify our model, we assume that all vehicles are plugged in whenever parked at home. We consider that plugging in the vehicle daily might not be a significant burden for users, especially if they could derive tangible benefits from participating in smart charging programs.
- All vehicles are charged until maximum state of energy (SOE) is reached, or the highest possible SOE that can be reached during the time the vehicle is plugged in.
- The battery capacity of all vehicles is 75 kWh, which is similar to that of the Tesla Model S [59].
- As per IEC 61851-1:2017 standard, we consider a Level 2 charger with a mean power rating of 7.4 kW, typically used for home charging [60].
- The charging efficiency η is 95% which is within the efficiency range of a Level 2 charger [61].

4.2. EV flexibility data

As input for the optimization process, we generate multiple flexibility forecasts for the EV fleet, distinguishing between forecasts for the DA period and the ID period. These forecasts depend on individual EV flexibility metrics (see Section 4.1). Specifically, we construct linear combinations of the 200 individual EV flexibility metrics (see Section 4.1). Each aggregated flexibility metric incorporates variables $E_t^{\min}$, $E_t^{\max}$, $P_t^{\min}$, $P_t^{\max}$, and E_t^{left}. The computational approach remains consistent across all variables, thus we present equations only for $E_t^{\min}$. For the DA period, we use a single aggregated flexibility metric computed using Eq. (19):

$$E_t^{\min,\text{DA}} = \sum_{v=1}^{200} w_v \times E_{t,v}^{\min} \quad \forall t \in T, \tag{19}$$

Here, the individual vehicle weight $w_v = 5$ holds for all vehicles (v), leading to an aggregated flexibility metric for 1000 EVs (200 × 5). In other words, we assume that the fleet of 1000 EVs has five types of EV, of which there are 200 each. For the ID period, we introduce variations by altering the weights associated with individual EV flexibility metrics, following Eq. (20):

$$E_t^{\min,\text{ID}} = \sum_{v=1}^{200} \text{round}(\tilde{w}_v) \times E_{t,v}^{\min} \quad \forall t \in T, \tag{20}$$

with $\tilde{w}_v \sim \mathcal{N}(\mu = 5, \sigma^2)$ truncated to $[-0.4\bar{9}, 10.4\bar{9}]$ for $\forall v$. Since individual EV metrics represent discrete users, we round the weights to integers. Truncation guarantees that the values of the final weights ($\tilde{w}$) are non-negative and less than or equal to ten, thus obtaining a symmetrical distribution of weights. The degree of divergence from the DA schedule increases with higher variance σ^2 in the truncated normal distribution.

After drawing weights from the distribution, we correct them to achieve unbiased power consumption estimates in the specific ID and DA schedules. Mathematically, we minimize the difference between the energy consumption in the DA and ID periods (see Eq. (21)):

$$\min_{\tilde{w}_v} \left| \sum_t E_t^{\text{left,ID}} - \sum_t E_t^{\text{left,DA}} \right|, \tag{21}$$

where, $\sum_t E_t^{\text{left,ID}}$ and $\sum_t E_t^{\text{left,DA}}$ represent the total energy consumption in the ID and DA schedules, respectively. Long-term lack of bias requires there to be no overestimation nor underestimation of power consumption occurring throughout the simulation. This is an important factor for schedules which are used as forecasts for power procurement.

4.3. Price data

Our study uses various historical price datasets, using the German market as a reference: DA auction prices, CID market transactions, and reBAPs. We obtain all DA and CID market data from EPEX [24] and focus solely on hourly product price data. For the DA market, we directly use auction clearing prices. However, handling CID market data is more complex due to the large number and random timing of trades. As a solution, we calculate volume-weighted average prices (VWAPs) at different intervals.

We generate two types of VWAPs for calculating the price forecasts and transaction prices during CID optimization. For forecasting, we calculate backward-looking price averages aligning with the efficient market hypothesis, which states that current asset prices reflect available information at any given time [62]. More specifically, we use the average price of the four most recent completed trades, as this method has demonstrated strong forecasting accuracy across various forecasting horizons [16]. Within the CID market context, this implies that the latest transaction prices are indicative of the most up-to-date information available. For ex-post price calculation, we employ forward-looking quarter-hourly VWAPs. Although market liquidity is generally high, there is no guarantee that trades occur for a product during every considered interval, potentially leading to situations where orders remain uncleared. To address this, we use a backfilling approach, relying on future prices to fill these gaps. While this method introduces a delay in the timing of specific transactions, the trades are still executed, ensuring that the simulation results remain valid. Meanwhile, for CID prices, we also use a VWAP, considering trades between one hour and half an hour before delivery, known as ID_1 and available from EPEX since 2021 [18]. For periods predating 2021, we compute our own ID_1 index. For trades in the CID market, we assume a volume trading fee of 0.1€/MWh [63].

Lastly, we obtain reBAP prices from TransnetBW [64] up to 2022 and Netztransparentz.de [65] starting from 2023. Since reBAP prices are quarter-hourly [17] and our study focuses on hourly products, we average the quarter-hourly prices to derive hourly prices.

5. Scenarios

We run our optimization across different scenarios defined by several dimensions. Section 5.1 presents the time frames, specifically the time period used for testing. Section 5.2 contains the parameterizations for the uncertainty modeling of EV flexibility. Section 5.3 covers the parameterization of the different trading strategies.

5.1. Timeframe

The study focuses on two specific time frames: the years 2019 and 2022. The year 2019 is chosen as it precedes both the Covid-19 pandemic and the Ukraine war, events that significantly impacted electricity markets [66]. In contrast, we include 2022 due to the heightened market price volatility in this year [66]. Examining periods of high price volatility contributes to the evaluation of the resilience of trading strategies under atypical market conditions. In our study, the EV schedules follow weekly patterns, requiring us to adjust the time intervals to start on the first Monday of the relevant year. For scenarios set in 2019, the specific dates range from January 2, 2019, to January 1, 2020. Similarly, for the 2022 scenarios, the time frame extends from January 5, 2022, to January 4, 2023.

5.2. EV uncertainty parameterization

We examine multiple forecasting scenarios for EVs. We employ the same DA flexibility metrics across all scenarios and generate a collection of ID flexibility metrics, each varying to a certain degree from the DA schedule. Section 4.2 elaborates on the method we use to create these flexibility metrics, based on individual EV profiles. We consider four different scenarios with increasing deviation between the DA and ID metrics, each characterized by a distinct standard deviation σ used for the distribution of the weights of individual EV metrics $\tilde{w}_v$:

1. Perfect forecast: $\sigma = 0$
2. Low deviation: $\sigma = 1$
3. Medium deviation: $\sigma = 2$
4. High deviation: $\sigma = 3$

Appendix B contains a more detailed evaluation of EV flexibility metrics. To obtain robust results, we repeat the calculations 128 times. The reason to do this is that we generate the aggregated ID flexibility metrics randomly. We selected 128 repetitions to match the hardware on which we carry out the computations: a high performance computing (HPC) node with two physical sockets, each containing an AMD Epyc ROME 7H12 processor with 64 cores, resulting in a total of 128 cores per node [67]. This hardware configuration enables the parallel execution of all scenarios.

Table 4
Trading strategies.

Strategy	Description	Section	Parameters
BL_P^{reBAP}	Baseline strategy with settlement of volumes for reBAP	3.3.1	N/A
$BL_P^{\text{ID}_1}$	Static CID strategy with settlement of volumes for ID_1	3.3.2	N/A
CID_E^x	Dynamic CID strategy with continuous settlement of volumes in CID market	3.3.3	x∈{2 min, 5 min, 10 min, 15 min, 20 min, 30 min, 60 min}

5.3. Trading strategies

We investigate various trading strategies for power settlement in the ID period. While the volumes acquired in the DA market stay constant across all trading strategies, we assess three unique trading strategies for rescheduling in response to the ID updates to EV schedules. Table 4 contains an overview of these strategies. The first two strategies (BL_P^{reBAP} and $BL_P^{\text{ID}_1}$) aim to closely align the ID schedule (P_t^{ID}) with the DA power schedule (P_t^{DA})(see Sections 3.3.1 and 3.3.2). However, these two strategies settle the discrepancies in the power schedules differently. The first strategy (BL_P^{reBAP}) settles power volumes as imbalances for the reBAP and the second strategy ($BL_P^{\text{ID}_1}$) settles power volumes in the CID market for the ID_1 price, which is a VWAP covering the period from one hour to half an hour before the start of delivery. Our third trading strategy (CID_E^x), operates continuously in the CID market and has different parametrizations (see Section 3.3.3). More specifically, these parameters define the hourly frequency at which the strategy runs, as defined by the period length (x) between single runs. We consider seven different such period lengths (x): 2 min, 5 min, 10 min, 15 min, 20 min, 30 min, and 60 min, which means that the optimization runs between thirty times and once per hour.

Our analysis evaluates the three trading strategies across two distinct periods, specifically the years 2019 and 2022 (see Section 5.1). Furthermore, we assess each strategy under a range of different EV flexibility uncertainties (see Section 5.2). We structure the analysis of our optimization strategies around the different trading strategies.

6. Results and discussion

This study introduces optimization models for EV scheduling in both DA and ID markets. In particular, our study focuses on the rescheduling of DA schedules during the ID period, taking account of price and EV user uncertainties. Section 6.1 illustrates the rescheduling process across the DA and ID time periods by discussing an exemplary period. Section 6.2, compares the different trading strategies, calculating the annual profit derived from trading EV flexibility in ID markets. Section 6.3 broadens the scope of comparison by evaluating the different trading strategies.

6.1. Rescheduling example

To illustrate the rescheduling process, we present results for an exemplary period of three days: June 6 to June 8, 2022. Each step contains flexibility metrics and schedules for power and energy respectively. The power schedule corresponds to the power purchased from the respective power markets. The energy schedule is the cumulative energy of all EVs connected to the grid. At any time, the power and energy schedules must stay between the bounds determined by the flexibility metrics, i.e., $P_t^{\min}$ and $P_t^{\max}$ for the power procured from market and $E_t^{\min}$ and $E_t^{\max}$ for the cumulative energy.

Fig. 5 contains the results of the DA optimization step (see Section 3.2). The DA energy and power schedules (E_t^{DA} and P_t^{DA}) are

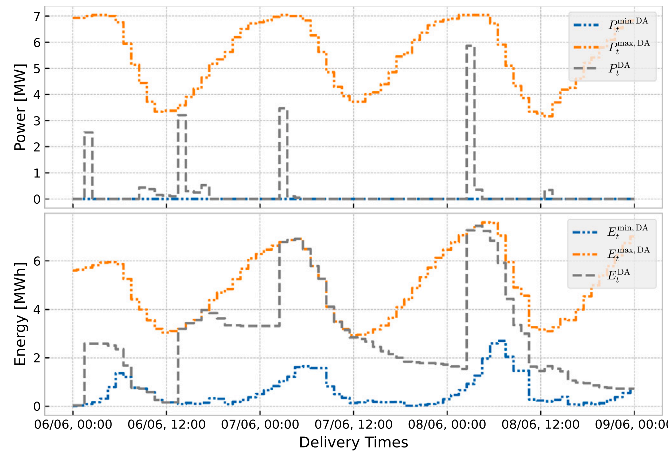

Fig. 5. Exemplary DA schedule for EV fleet from June 6 to June 8, 2022.

depicted as dashed lines (in gray), whereas the flexibility metrics are in the form of lower ($E_t^{\min,\text{DA}}$, $P_t^{\min,\text{DA}}$) and upper bounds ($E_t^{\max,\text{DA}}$, $P_t^{\max,\text{DA}}$) are shown as dashed lines with double dots (blue and orange respectively). The DA schedule (P_t^{DA}, E_t^{DA}) always stays between the limits defined by the flexibility metrics. The power schedule (P_t^{DA}) never reaches the upper limit and often takes the value of its lower limit ($P_t^{\min,\text{DA}}$) which is zero. In contrast, the energy schedule (E_t^{DA}) reaches both the bottom and the top limit, for example on June 6 during the intervals of 8:00–13:00 and 14:00–17:00 respectively. The DA schedule (E_t^{DA}, P_t^{DA}) serve as the starting points for the subsequent ID optimizations, for which the paper covers three options: a baseline strategy (see Section 3.3.1), a static CID strategy (see Section 3.3.2), and a dynamic CID strategy (see Section 3.3.3). Note that both the baseline strategy and the static CID strategy produce identical power and energy schedules, as neither incorporates price signals during rescheduling.

Fig. 6 illustrates the rescheduling in the ID period by the baseline strategy (or the static CID strategy), extending Fig. 5. In addition to the DA flexibility metrics and schedules, it additionally contains the ID flexibility metrics and the baseline ID schedule. The lower ($E_t^{\min,\text{ID}}$, $P_t^{\min,\text{ID}}$) and upper bounds ($E_t^{\max,\text{ID}}$, $P_t^{\max,\text{ID}}$) are dashed lines with double dots (green and red respectively); and the ID baseline schedule (P_t^{BL}, E_t^{BL}) is the dashdot line (black). Similar to the DA case, the baseline ID schedule remains within the boundaries defined by the ID flexibility metrics. More specifically, the power schedule (P_t^{BL}) never reaches its upper limit, while the energy schedule (E_t^{BL}) reaches both the upper and the lower limits.

Fig. 7 exemplifies the dynamic CID rescheduling by extending Fig. 5. Just as for the baseline rescheduling, the figure contains the ID bounds. In addition, it also contains the final ID schedule for a CID optimization (E_t^{CID}, P_t^{CID}) with 15 min trading frequency as dashdot line (cyan). Similarly to the DA and baseline cases, the CID schedule (E_t^{CID}, P_t^{CID}) stays within the bounds set by the ID flexibility metrics, where the power schedule (P_t^{CID}) mostly follows the lower bound ($P_t^{\min,\text{ID}}$) and the energy schedule reaches both the lower and the higher energy bounds ($E_t^{\min,\text{ID}}$ and $E_t^{\max,\text{ID}}$).

Taking a closer look at Fig. 6 or Fig. 7, we observe that the DA schedule violates the ID bounds. Note that the ID flexibility metrics are the same in both figures. For example, on June 6 at 14:00–18:00 the DA energy schedule (E_t^{DA}) violates the ID upper energy boundary ($E_t^{\max,\text{ID}}$). This violation highlights the need for rescheduling the DA schedule to comply with the ID boundaries.

We discuss two distinct rescheduling approaches: the baseline (or static CID) rescheduling (see Fig. 6) and the CID trading strategy (see Fig. 7). The core difference between these approaches lies in their power schedules. The baseline strategy and static CID strategy (see

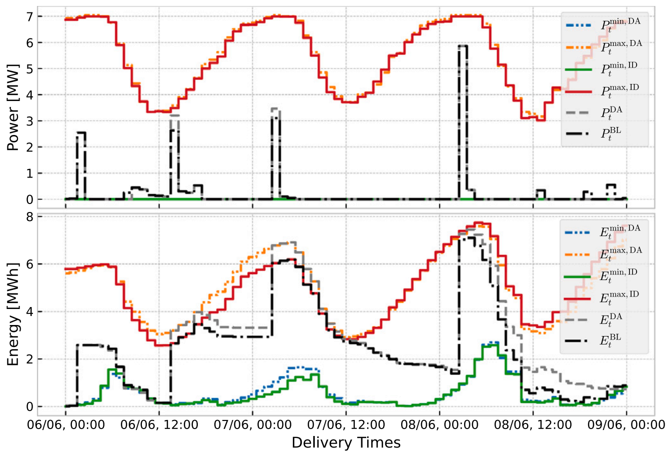

Fig. 6. Exemplary baseline schedule for EV fleet from June 6 to June 8, 2022.

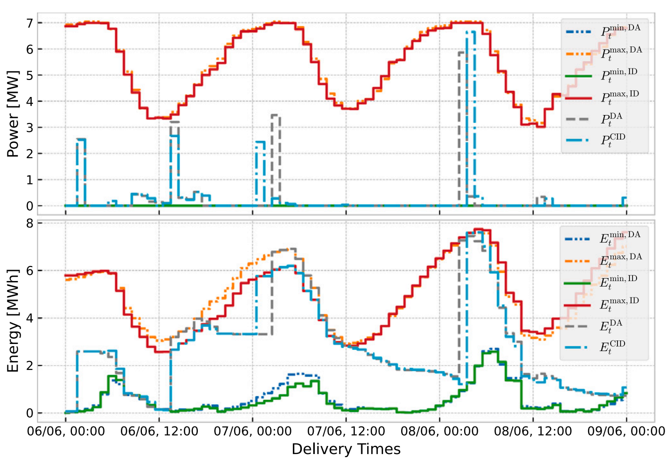

Fig. 7. Exemplary CID final schedule for EV fleet from June 6 to June 8, 2022.

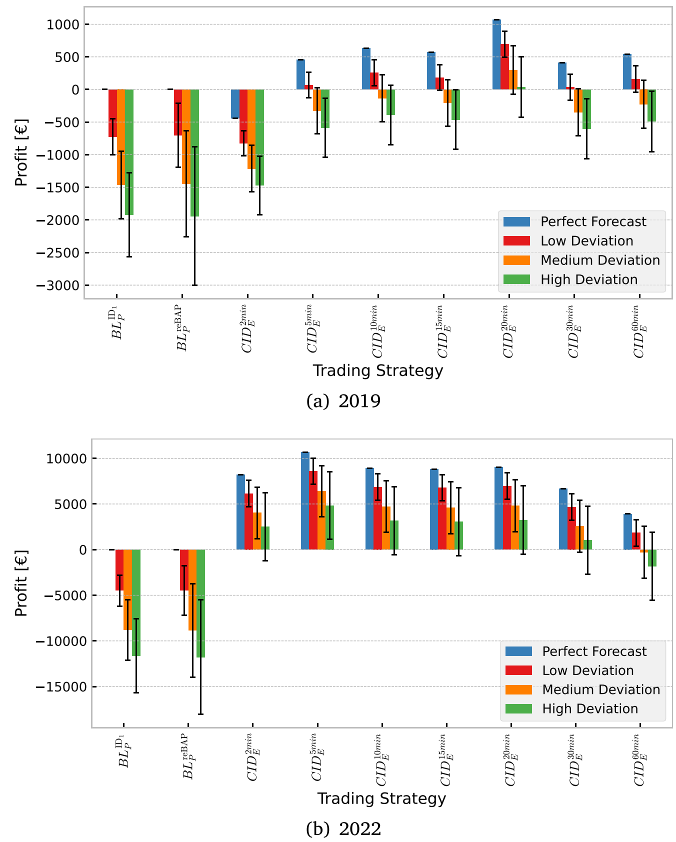

Fig. 8. Comparison of yearly profits for different trading strategies in 2019 and 2022.

Fig. 6) aim to minimize trading volumes. Therefore, they selects a power schedule that tracks closely the DA schedule (E_t^{DA}). As a result, the resulting power schedule (P_t^{BL}) predominantly adjusts the power magnitude, while maintaining the original timing of the DA power schedule (P_t^{DA}). An instance of such an adjustment occurs on June 7 at 3:00. In contrast, the power schedule of the dynamic CID strategy (P_t^{CID}) deviates significantly from the DA power schedule (P_t^{DA}) in both timing and magnitude (see Fig. 7). For example, this deviation can be seen on June 7 where the optimization shifts power from 3:00 in DA to 1:00 in CID. The different rescheduling results are a consequence of the strategy's dual objectives: to adhere to ID constraints and to capitalize on price arbitrage opportunities. Consequently, the times when charging power is scheduled differ between the DA and ID schedules. This leads to situations where EVs end up being charged at different times under the ID schedule compared to what was originally planned in the DA period.

To sum up, all strategies successfully adjust their schedules to stay within the ID energy and power constraints. However, the differences in their power schedules highlight their different optimization targets.

6.2. Trading profit

The financial evaluation of the rescheduling strategies involves calculating the expected yearly profits for 1000 EVs under each strategy. For each strategy, we compute the annual profits during the ID period by aggregating the value of all transactions occurring within this period. This includes all trades in the CID including CID fees and imbalance settlement costs. More precisely, under the assumption of positive prices, profit rises when selling power volumes and declines when acquiring power volumes. Conversely, when prices are negative, the profit directions invert. The optimization algorithms behind the strategies operate without knowledge of future prices. They rely on price forecasts. However, the computation of profit uses actual prices for both the CID and imbalances, namely the reBAP. We analyze the two years 2019 and 2022 separately due to different market conditions, yielding two sets of profits.

The bar charts in Fig. 8 illustrates the mean annual profits generated by the various trading strategies. The chart contains four bars for each strategy, with each bar representing a different level of discrepancy between the DA and ID EV flexibility forecasts. From left to right the bars represent a perfect forecast (in blue), low deviation (in orange), a medium deviation (in green), and high deviation (in red) (see Sections 4.2 and 5.2 for more details on EV flexibility forecasts). To provide information on the variability of profit, each bar includes whiskers that extend to show a range of two standard deviations above and below the average profit. The strategies BL_P^{reBAP} and $BL_P^{\mathrm{ID}_1}$ only vary in their power volume clearing approach. The strategy BL_P^{reBAP} takes power volumes to the imbalance market, clearing for the reBAP, and $BL_P^{\mathrm{ID}_1}$ trades in the CID market clearing for the ID_1 price. The range of strategies from CID_E^{2min} to CID_E^{60min} represent different parametrizations of the dynamic CID strategy, distinguished by their decision frequency intervals, specifically 2 min and 60 min in the mentioned strategies, as described in Sections 3.3.3 and 5.3.

Analyzing the strategies employed during these two years, we observe a consistent trend across all strategies. Profit declines noticeably as the deviation between the DA and ID EV flexibility forecasts increases. Further, the decline of profit correlates with an increase in profit variability, as indicated by the expanding whisker intervals. This trend occurs since larger deviations between the DA and ID EV flexibility forecasts necessitate more involuntary rescheduling. The term "involuntary rescheduling" refers to rescheduling due to violations of ID flexibility metrics, in contrast to "voluntary rescheduling", which occurs exclusively to enhance profit through arbitrage. The occurrence of involuntary rescheduling reduces the flexibility available for voluntary rescheduling, thereby reducing the potential and increasing the volatility of profits.

Focusing on the baseline strategy and the static CID strategy, namely $BL_P^{\mathrm{ID}_1}$ and BL_P^{reBAP}, the strategies yield zero profit in the perfect forecast scenario. This outcome is a consequence of their design, which minimizes traded volumes. In other words, when forecasts are perfect, these strategies do not engage in trading, leading to the generation of neutral profits. However, the profits from these strategies become increasingly negative in the scenarios with higher deviation between the DA and ID EV flexibility forecasts. These negative profits are a consequence of involuntary rescheduling and limited exploitation of EV flexibility inherent to these strategies, as they only adapt schedules to ID flexibility metrics.

In contrast, the outcomes for the dynamic CID strategies are more favorable. These strategies (ranging from CID_E^{2min} to CID_E^{60min}), do not only adjust positions to comply with the ID flexibility constraints, but they also exploit arbitrage opportunities when trading across different products. In the year 2019, only the CID_E^{20min} strategy yields positive profits across all levels of deviation, reaching up to €1,067.98. The year 2022 has different characteristics, with all CID strategies except CID_E^{60min} generating positive profits at all deviation levels. Notably, the overall profit in 2022 is significantly higher. The top-performing strategy CID_E^{5min} reaches profit of up to €10,670.59.

The comparison of the results from 2019 and 2022 reveals two differences. First, profit margins vary significantly between the two years, being significantly higher in 2022. This rise reflects the differing market conditions, particularly the higher prices in 2022 and the ensuing rise in volatility. Secondly, the optimal dynamic CID strategy differed between the years. In 2019, the CID_E^{20min} strategy performs best, whereas in 2022, the CID_E^{5min} strategy performs best. The strategies differ in their trading frequency (every 5 min as opposed to every 20 min). This difference indicates that a higher trading frequency was beneficial in 2022, contrary to 2019. This finding contradicts the expectation that higher frequency trading should yield more profit by revealing a greater arbitrage opportunities. However, market liquidity is limited and changes over time. Markets in 2019 were less liquid than those in 2022. The increase in CID market liquidity from 2019 to 2022 provides a plausible explanation for the shift towards a higher optimal trading frequency.

In summary, the analysis over two years reveals that trading profit decreases with downgrades of EV flexibility forecasts. The baseline strategy and the static CID strategy minimize traded volumes, and therefore yield no profits under perfect forecasts, and lead to losses with greater forecast deviations. In contrast, dynamic CID strategies can incur profits, with higher frequency CID trading strategies being more profitable in 2022 than in 2019. Overall margins are significantly higher in 2022 than in 2019. Additionally, the results underscore the importance of accurate EV flexibility forecasts, and the need for trading to adapt to market conditions.

6.3. Trading profits over imbalance baseline

Expanding our analysis, we evaluate the relative profitability of strategies trading in the CID market against the baseline strategy (BL_P^{reBAP}) that takes volumes to the imbalance market and incurs the reBAP. Consideration of relative profits enables us to illustrate the financial implications of participating in the CID market, as opposed to settling volumes as imbalances which incur the reBAP price.

Fig. 9 displays differences in profits of the 1000 EVs for all strategies trading in the CID ($BL_P^{\mathrm{ID}_1}$, and CID_E^{2min} to CID_E^{60min}) over the baseline

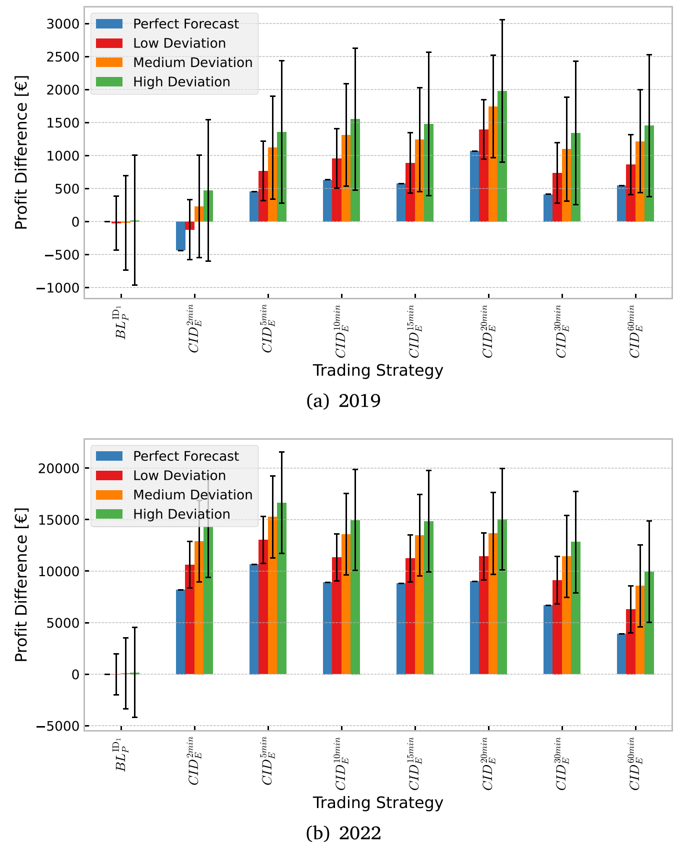

Fig. 9. Comparison of yearly improvement over BL_P^{reBAP} as a share of DA costs in 2019 and 2022.

strategy BL_P^{reBAP}. To represent uncertainty, each bar has whiskers that extend two standard deviations above and below the mean profit differences. Echoing the approach in Fig. 8, Fig. 9 also displays results for different levels of deviation between the DA and ID flexibility forecasts. It also features two plots, one for each of the years 2019 and 2022.

Comparing the various strategies, the static CID strategy $BL_P^{\mathrm{ID}_1}$, which settles volumes at the ID_1 price, performs similarly to the baseline strategy (BL_P^{reBAP}), as indicated by the approximate zero values in the figure. Within the dynamic CID strategies, the most yield an improvement over the static CID strategy $BL_P^{\mathrm{ID}_1}$ in both 2019 and 2022. A singular exception is the CID_E^{2min} strategy under the perfect forecast scenario in 2019, which under-performs relative to the baseline strategy, a fact underscored by the negative values on the graph. Conversely, all other dynamic CID strategies show gains over the baseline strategy, suggesting that energy suppliers would benefit from adopting these strategies rather than depending on the baseline strategy and settling additional power needs in imbalance markets. The extent of these improvements increases with the level of deviation between the DA and ID schedules.

The increased benefit of participating in the CID market under conditions of higher uncertainty in EV schedules arises from the dynamic CID strategy being able to facilitate the exploitation of EV charging flexibility for arbitrage across products with different delivery intervals. Our dynamic CID trading strategy capitalizes efficiently on these arbitrage opportunities. EV charging is particularly suitable for such optimization. Given the constraints set by user requirements, the charging intervals can be optimized not only to reduce imbalances, but also to generate profit.

6.4. Limitations and outlook

We acknowledge limitations in our study that open avenues for future research. Although we focused on the German market, our methodology could be adapted to other European markets due to the harmonization of power market designs [68]. Incorporating additional market segments like the IDA could provide more trading opportunities. Applying cross-market optimization instead of sequential optimization might increase profits and allow for the selection of the most favorable prices. Future research could explore the optimal distribution of purchase volumes across various markets in a multi-market optimization framework, though this requires advanced price forecasts beyond our current scope.

Enhancing CID price forecasting models and increasing the temporal resolution of products to 15-minute intervals could improve profitability and provide more granular insights. Our assumption that ID EV flexibility forecasts equal realized flexibility stems from the fact that the ID forecasting time is very close to the actual realization and that we are considering a fleet of EVs. However, this assumption requires further investigation, as there may still be discrepancies between forecasts and actual flexibility.

To quantify EV flexibility in our paper, we use synthetic data generated from the German mobility patterns. While this approach is effective, it may overlook certain uncertainties in driving and charging behaviors. For instance, mobility patterns in Germany could shift during the holiday season—a detail that synthetic data may not fully capture. Future research could use real-world data to quantify EV flexibility, allowing for a more precise modeling of such seasonal variations and behavioral uncertainties. Additionally, we assume linear charging for simplicity. In reality, charging power decreases when the state of charge (SOC) of the battery is getting closer to full battery capacity, which can extend charging times and might reduce flexibility. Despite this, aggregating multiple EVs helps minimize the individual discrepancies, so the impact on overall profits from trading EV flexibility in the CID market remains relatively small. Finally, while our current model assumes full flexibility provision by EV users, exploring scenarios with partial flexibility provision is essential for understanding the strategies' applicability.

7. Conclusion

In this paper we explored the potential of EV charging flexibility trading in the CID market. Our focus was twofold: examining market price dynamics in the CID market, and the uncertainties caused by unpredictable EV user behavior. To address CID price uncertainties, we used a forecasting model to inform trading decisions. When considering the uncertainties of EV charging requirements, we took account of a DA forecast, which later underwent an update with a new forecast made during the ID period.

Our method involved a two-step optimization process. First, we optimized power acquisition in the DA market according to the DA EV charging flexibility forecast. Second, based on an updated ID EV flexibility forecast, we reoptimized the charging schedules. We introduced several trading strategies for this readjustment. The baseline strategy avoids completely any trading in the CID market, opting instead to always settle imbalances through the reBAP. In contrast, our alternative strategies settle power volumes directly in the CID market. We paid special attention to strategies that exploit EV charging flexibility, as these feature arbitrage opportunities within the CID market. We also explored rolling windows with their different trading frequencies.

The empirical results suggest that higher differences in EV charging flexibility metrics between the DA and ID coincide with decreased profits across all examined strategies. Nonetheless, the advantage of trading in the CID market increases with greater EV charging schedule uncertainty. Active trading in CID markets improves profit margins, as this creates market arbitrage opportunities by exploiting EVs' charging flexibility. Adhering to a baseline strategy and clearing the remaining power differences through imbalance markets incurs considerable costs. Our optimization method can facilitate more successful trading in the CID market, thus helping to manage forecast discrepancies in EV schedules and potentially generating profits. In our scenario with the highest deviation between the DA and ID flexibility metrics, applying the best CID strategies yielded an average yearly profit of €37.52 and €4,840.63 for 1000 EVs in 2019 and 2022 respectively. In comparison to the baseline strategy, which clears volumes as imbalances, the corresponding financial savings amounted to €1,978.52 and €16,632.25 respectively.

Our findings suggest that with an appropriate trading strategy, energy suppliers serving EV users can mitigate financial risks arising from inaccuracies in the forecasts of EV power requirements. The efficacy of such a strategy relies on two key components: First, it requires EV users to facilitate flexibility, specifically through the adoption of smart charging practices. Second, it requires strategic trading in the CID market. A profitable trading strategy should not only take account of the flexibility offered by EVs, but should also feature arbitrage between products that are traded in parallel.

CRediT authorship contribution statement

Raviteja Chemudupaty: Writing – review & editing, Writing – original draft, Visualization, Software, Methodology, Data curation, Conceptualization. **Timothée Hornek:** Writing – review & editing, Writing – original draft, Visualization, Software, Methodology, Data curation, Conceptualization. **Ivan Pavić:** Writing – review & editing, Conceptualization. **Sergio Potenciano Menci:** Writing – review & editing.

Declaration of Generative AI and AI-assisted technologies in the writing process

During the preparation of this work the authors used ChatGPT and Writefull in order to improve readability and language. After using this tool/service, the authors reviewed and edited the content as needed and take full responsibility for the content of the publication.

Declaration of competing interest

The authors declare the following financial interests/personal relationships which may be considered as potential competing interests: Raviteja Chemudupaty reports financial support was provided by Fondation Enovos. Timothee Hornek reports financial support was provided by Enovos Luxembourg S.A. Ivan Pavic reports financial support was provided by Enovos Luxembourg S.A. Sergio Potenciano Menci reports financial support was provided by Luxembourg National Research Fund. If there are other authors, they declare that they have no known competing financial interests or personal relationships that could have appeared to influence the work reported in this paper.

Acknowledgments

This research was funded in part by the Luxembourg National Research Fund (FNR) and PayPal, PEARL grant reference 13342933/Gilbert Fridgen. This research was funded in part by the Luxembourg National Research Fund (FNR), grant reference 17886330. For the purpose of open access, and in fulfillment of the obligations arising from the grant agreement , the author has applied a Creative Commons Attribution 4.0 International (CC BY 4.0) license to any Author Accepted Manuscript version arising from this submission.

The authors gratefully acknowledge the Fondation Enovos under the aegis of the Fondation de Luxembourg in the frame of the philanthropic funding for the research project INDUCTIVE which is the initiator of this applied research.

The research was carried out as part of a partnership with the energy retailer Enovos Luxembourg S.A.

Appendix A. Absolute values in LP objective functions

Objective functions containing absolute values are not inherently solvable by a linear programming (LP) solvers. However, in specific scenarios, these objective functions can be linearized. Consider the objective function expressed in Eq. (A.1):

$$\min \sum_i |a_i - b_i|, \tag{A.1}$$

where a_i and b_i represent variables, potentially subject to linear constraints. Linearizing this objective function involves introducing auxiliary variables ($z_i \forall i$) alongside additional constraints (see Eqs. (A.3) and (A.4)). The modified optimization problem is defined by the objective function in Eq. (A.2):

$$\min \sum_i z_i, \tag{A.2}$$

subject to the new constraints:

$$z_i \geq a_i - b_i \quad \forall i, \tag{A.3}$$

$$z_i \geq b_i - a_i \quad \forall i, \tag{A.4}$$

in addition to the original problem's constraints. This reformulation aligns with an LP formulation. Note that this transformation is applicable exclusively to minimization problems.

Appendix B. Aggregated EV flexibility evaluation

To validate the parameterization of the resulting schedules, we quantify the deviation between the DA and ID schedules using two established error metrics: the root mean squared error (RMSE) and the mean absolute error (MAE). For instance, the respective metric definitions for $E_t^{\min}$ are given by:

$$MAE(E_t^{\min}) = \frac{1}{|T|} \sum_{t \in T} \left| E_t^{\min,\mathrm{ID}} - E_t^{\min,\mathrm{DA}} \right| \tag{B.1}$$

$$RMSE(E_t^{\min}) = \sqrt{\frac{1}{|T|} \sum_{t \in T} \left(E_t^{\min,\mathrm{ID}} - E_t^{\min,\mathrm{DA}} \right)^2}, \tag{B.2}$$

where $E_t^{\min,\mathrm{ID}}$ denotes the ID bound for $E_t^{\min}$, while $E_t^{\min,\mathrm{DA}}$ denotes the DA bound for $E_t^{\min}$. The same definition applies to: $E_t^{\min}$, $E_t^{\max}$, $P_t^{\max}$, and E_t^{left}. We omit $P_t^{\min}$ from further consideration as we assume that $P_t^{\min,\mathrm{DA}} = P_t^{\min,\mathrm{ID}} = 0$, implying that both RMSE and MAE yield errors of zero.

Fig. B.10 depicts the resulting error metric values for the low, medium, and high deviations between the DA and ID flexibility metrics (see Section 3.1.3). Table B.5 contains the exact values depicted in Fig. B.10. We omit the results for the perfect forecast scenario in the figure, since all errors are zero. In the figure, the whiskers span two standard deviations both above and below the mean, meaning that, if we assume normality of the errors, the whiskers cover over 95% of the target population.

Comparing the different variables, both the RMSE and MAE errors for the maximum energy level $E_t^{\max}$ exceed the errors of the other variables. This implies, that the maximum energy level $E_t^{\max}$ is most sensitive to forecast errors in EV user behavior. Comparing the different scenarios yields a consistent pattern across variables. The errors for the variables increase in line with the deviation level between the DA and ID schedules, validating our generation approach for the schedule bounds.

Data availability

The authors do not have permission to share data.

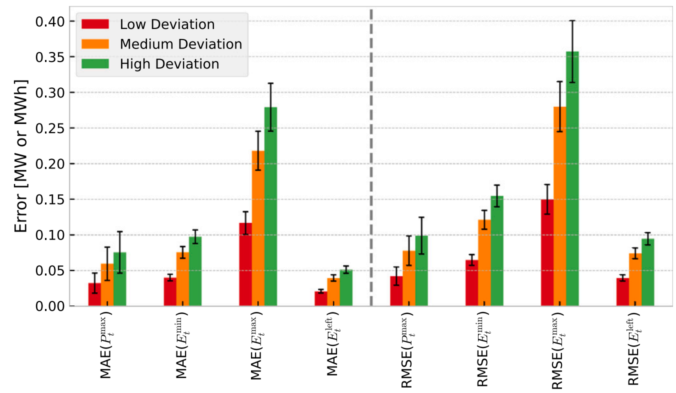

Fig. B.10. Mean absolute percentage error (MAPE) and root mean squared percentage error (RMSPE) for the different flexibility metrics.

Table B.5
Means and standard deviations of relative errors of EV schedule variables for different levels of deviations EV flexibility forecast deviations in %.

(a) 2019

Strategy	Mean			Std.		
	Low	Medium	High	Low	Medium	High
MAE($P_t^{\max}$)	3.23	5.94	7.54	0.71	1.16	1.45
MAE($E_t^{\min}$)	4.0	7.54	9.73	0.23	0.41	0.48
MAE($E_t^{\max}$)	11.67	21.8	27.91	0.8	1.37	1.68
MAE(E_t^{left})	2.08	3.95	5.12	0.12	0.22	0.25
RMSE($P_t^{\max}$)	4.22	7.78	9.9	0.64	1.03	1.29
RMSE($E_t^{\min}$)	6.47	12.11	15.46	0.38	0.66	0.76
RMSE($E_t^{\max}$)	14.98	27.99	35.73	1.04	1.76	2.17
RMSE(E_t^{left})	3.96	7.41	9.45	0.22	0.38	0.43

(b) 2022

Strategy	Mean			Std.		
	Low	Medium	High	Low	Medium	High
MAE($P_t^{\max}$)	3.22	5.92	7.57	0.67	1.18	1.48
MAE($E_t^{\min}$)	4.01	7.52	9.71	0.22	0.41	0.45
MAE($E_t^{\max}$)	11.66	21.77	27.89	0.74	1.4	1.58
MAE(E_t^{left})	2.08	3.94	5.11	0.12	0.22	0.25
RMSE($P_t^{\max}$)	4.2	7.76	9.92	0.6	1.05	1.3
RMSE($E_t^{\min}$)	6.48	12.08	15.43	0.36	0.68	0.73
RMSE($E_t^{\max}$)	14.98	27.95	35.7	0.98	1.81	2.06
RMSE(E_t^{left})	3.96	7.39	9.44	0.21	0.39	0.42

References

[1] International Energy Agency. Global EV outlook 2023: catching up with climate ambitions, global EV outlook. OECD; 2023, http://dx.doi.org/10.1787/cbe724e8-en, URL: https://www.oecd-ilibrary.org/energy/global-ev-outlook-2023_cbe724e8-en.

[2] Ajanovic A, Haas R. Electric vehicles: solution or new problem? Environ Dev Sustain 2018;20:7–22. http://dx.doi.org/10.1007/s10668-018-0190-3.

[3] Daina N, Sivakumar A, Polak JW. Modelling electric vehicles use: a survey on the methods. Renew Sustain Energy Rev 2017;68:447–60. http://dx.doi.org/10.1016/j.rser.2016.10.005, URL: https://linkinghub.elsevier.com/retrieve/pii/S1364032116306566.

[4] Pareschi G, Küng L, Georges G, Boulouchos K. Are travel surveys a good basis for EV models? Validation of simulated charging profiles against empirical data. Appl Energy 2020;275:115318. http://dx.doi.org/10.1016/j.apenergy.2020.115318, URL: https://www.sciencedirect.com/science/article/pii/S0306261920308308.

[5] KLE Institute. EI fact sheet: the current electricity market design in Europe. Technical report, KU Leuven Energy Institute; 2015, URL: https://set.kuleuven.be/ei/images/EI_factsheet8_eng.pdf/.

[6] Eldeeb HH, Faddel S, Mohammed OA. Multi-objective optimization technique for the operation of grid tied PV powered EV charging station. Electr Power Syst Res 2018;164:201–11. http://dx.doi.org/10.1016/j.epsr.2018.08.004, URL: https://linkinghub.elsevier.com/retrieve/pii/S0378779618302475.
[7] Haupt L, Schöpf M, Wederhake L, Weibelzahl M. The influence of electric vehicle charging strategies on the sizing of electrical energy storage systems in charging hub microgrids. Appl Energy 2020;273:115231. http://dx.doi.org/10.1016/j.apenergy.2020.115231, URL: https://www.sciencedirect.com/science/article/pii/S0306261920307431.
[8] Raghavan SS. Impact of demand response on Electric Vehicle charging and day ahead market operations. In: 2016 IEEE power and energy conference at illinois. 2016, p. 1–7. http://dx.doi.org/10.1109/PECI.2016.7459218.
[9] Pavić I, Capuder T, Kuzle I. Value of flexible electric vehicles in providing spinning reserve services. Appl Energy 2015;157:60–74. http://dx.doi.org/10.1016/j.apenergy.2015.07.070, URL: https://www.sciencedirect.com/science/article/pii/S0306261915009101.
[10] Naharudinsyah I, Limmer S. Optimal charging of electric vehicles with trading on the intraday electricity market. Energies 2018;11:1416. http://dx.doi.org/10.3390/en11061416, URL: https://www.mdpi.com/1996-1073/11/6/1416, number: 6 Publisher: Multidisciplinary Digital Publishing Institute.
[11] Tepe B, Figgener J, Englberger S, Sauer DU, Jossen A, Hesse H. Optimal pool composition of commercial electric vehicles in V2G fleet operation of various electricity markets. Appl Energy 2022;308:118351. http://dx.doi.org/10.1016/j.apenergy.2021.118351, URL: https://www.sciencedirect.com/science/article/pii/S0306261921015981.
[12] Vardanyan Y, Madsen H. Optimal coordinated bidding of a profit maximizing, risk-averse EV aggregator in three-settlement markets under uncertainty. Energies 2019;12:1755. http://dx.doi.org/10.3390/en12091755, URL: https://www.mdpi.com/1996-1073/12/9/1755, number: 9 Publisher: Multidisciplinary Digital Publishing Institute.
[13] Shinde P, Kouveliotis-Lysikatos I, Amelin M, Song M. A modified progressive hedging approach for multistage intraday trade of EV aggregators. Electr Power Syst Res 2022;212:108518. http://dx.doi.org/10.1016/j.epsr.2022.108518, URL: https://www.sciencedirect.com/science/article/pii/S0378779622006307.
[14] Shinde P, Amelin M. A literature review of intraday electricity markets and prices. In: 2019 IEEE milan powertech. 2019, p. 1–6. http://dx.doi.org/10.1109/PTC.2019.8810752.
[15] Gaete-Morales C, Kramer H, Schill W-P, Zerrahn A. An open tool for creating battery-electric vehicle time series from empirical data, emobpy. Sci Data 2021;8:152. http://dx.doi.org/10.1038/s41597-021-00932-9, URL: http://www.nature.com/articles/s41597-021-00932-9.
[16] Hornek T, Potenciano Menci S, Delgado Fernández J, Pavić I. Comparative analysis of baseline models for rolling price forecasts in the german continuous intraday electricity market | energy proceedings. Energy Proc 2024;38. http://dx.doi.org/10.46855/energy-proceedings-10885, URL: https://www.energy-proceedings.org/comparative-analysis-of-baseline-models-for-rolling-price-forecasts-in-the-german-continuous-intraday-electricity-market/.
[17] HT GmbH, A GmbH, TT GmbH, T GmbH. Berechnung des regelzonenübergreifenden einheitlichen Bilanzausgleichsenergiepreises (reBAP). Technical report, 2022, URL: https://www.netztransparenz.de/xspproxy/api/staticfiles/ntp-relaunch/dokumente/regelenergie/ausgleichsenergiepreis/modellbeschreibung_der_rebap-berechnung_ab_08-12-2022.pdf.
[18] ES SE. Description of epex spot markets indices. Technical report, EPEX SPOT SE; 2023, URL: https://www.epexspot.com/sites/default/files/download_center_files/EPEX%20SPOT%20Indices%202019-05_final.pdf.
[19] ES SE. EPEX SPOT annual market review 2023. Technical report, EPEX SPOT SE; 2024, URL: https://www.epexspot.com/sites/default/files/download_center_files/2024-01-23_EPEX%20SPOT_Annual%20Press%20Release%202023_0.pdf.
[20] AN Committee. CACM annual report 2022. Technical report, All NEMO Committee; 2023, URL: https://www.nemo-committee.eu/assets/files/cacm-annual-report-2022.pdf.
[21] MCS Committee. SIDC stakeholder report October 2023. Technical report, Market Coupling Steering Committee; 2023, URL: https://www.nemo-committee.eu/assets/files/SIDC_stakeholder_report_1023-f284194310bdf658e82e27220a285de1.pdf.
[22] ES SE. Trading at EPEX SPOT. Technical report, EPEX SPOT SE; 2022, URL: https://www.epexspot.com/sites/default/files/2022-07/22-07-12_TradingBrochure.pdf.
[23] Zachmann G, Hirth L, Heussaff C, Schlecht I, Mühlenpfordt J, Eicke A. The design of the European electricity market - current proposals and ways ahead. Technical report, Policy Department for Economic, Scientific and Quality of Life Policies Directorate-General for Internal Policies; 2023, URL: https://www.europarl.europa.eu/RegData/etudes/STUD/2023/740094/IPOL_STU(2023)740094_EN.pdf.
[24] ES SE. Market data | EPEX SPOT. 2024, URL: https://www.epexspot.com/en/market-data.
[25] AN Committee. Single intraday coupling (XBID) information package. Technical report, All NEMO Committee; 2021, URL: https://www.nemo-committee.eu/assets/files/SIDC_Information%20Package_April%202021-99076f6ed5001c4d47442ae5cccebf30.pdf.
[26] Neuhoff K, Ritter N, Salah-Abou-El-Enien A, Vassilopoulos P. Intraday markets for power: Discretizing the continuous trading? SSRN Electr J 2016. http://dx.doi.org/10.2139/ssrn.2723902.
[27] ENTSO-E. ENTSO-E balancing report 2022. Technical report, ENTSO-E; 2022, URL: https://eepublicdownloads.entsoe.eu/clean-documents/nc-tasks/2022_ENTSO_E_Balancing_Report_Web_2bddb9ad4f.pdf.
[28] Foley A, Tyther B, Calnan P, Gallachóir BÓ. Impacts of Electric Vehicle charging under electricity market operations. Appl Energy 2013;101:93–102. http://dx.doi.org/10.1016/j.apenergy.2012.06.052, URL: https://linkinghub.elsevier.com/retrieve/pii/S0306261912004977.
[29] Okur O, Heijnen P, Lukszo Z. Aggregator's business models in residential and service sectors: A review of operational and financial aspects. Renew Sustain Energy Rev 2021;139:110702. http://dx.doi.org/10.1016/j.rser.2020.110702, URL: https://www.sciencedirect.com/science/article/pii/S1364032120309837.
[30] Li T, Tao S, He K, Lu M, Xie B, Yang B, et al. V2G multi-objective dispatching optimization strategy based on user behavior model. Front Energy Res 2021;9. URL: https://www.frontiersin.org/articles/10.3389/fenrg.2021.739527.
[31] Ayyadi S, Maaroufi M. Optimal framework to maximize the workplace charging station owner profit while compensating electric vehicles users. Math Probl Eng 2020;2020:1–12. http://dx.doi.org/10.1155/2020/7086032, URL: https://www.hindawi.com/journals/mpe/2020/7086032/.
[32] Rassaei F, Soh W-S, Chua K-C. A statistical modelling and analysis of residential electric vehicles' charging demand in smart grids. In: 2015 IEEE power & energy society innovative smart grid technologies conference. Washington, DC, USA: IEEE; 2015, p. 1–5. http://dx.doi.org/10.1109/ISGT.2015.7131894, URL: http://ieeexplore.ieee.org/document/7131894/.
[33] Gjelaj M, Arias NB, Traeholt C, Hashemi S. Multifunctional applications of batteries within fast-charging stations based on EV demand-prediction of the users' behaviour. J Eng 2019;2019:4869–73. http://dx.doi.org/10.1049/joe.2018.9280, URL: https://onlinelibrary.wiley.com/doi/10.1049/joe.2018.9280.
[34] Jin Y, Yu B, Seo M, Han S. Optimal aggregation design for massive V2G participation in energy market. IEEE Access 2020;8:211794–808. http://dx.doi.org/10.1109/ACCESS.2020.3039507.
[35] Iversen EB, Morales JM, Madsen H. Optimal charging of an electric vehicle using a Markov decision process. Appl Energy 2014;123:1–12. http://dx.doi.org/10.1016/j.apenergy.2014.02.003, URL: https://www.sciencedirect.com/science/article/pii/S0306261914001226.
[36] Sokorai P, Fleischhacker A, Lettner G, Auer H. Stochastic modeling of the charging behavior of electromobility. World Electr Veh J 2018;9:44. http://dx.doi.org/10.3390/wevj9030044, URL: https://www.mdpi.com/2032-6653/9/3/44. [number: 3 Publisher: Multidisciplinary Digital Publishing Institute].
[37] Müller M, Biedenbach F, Reinhard J. Development of an integrated simulation model for load and mobility profiles of private households. Energies 2020;13:3843. http://dx.doi.org/10.3390/en13153843, URL: https://www.mdpi.com/1996-1073/13/15/3843.
[38] Su J, Lie TT, Zamora R. Modelling of large-scale electric vehicles charging demand: A New Zealand case study. Electr Power Syst Res 2019;167:171–82. http://dx.doi.org/10.1016/j.epsr.2018.10.030, URL: https://www.sciencedirect.com/science/article/pii/S0378779618303535.
[39] Wang Z, Jochem P, Fichtner W. A scenario-based stochastic optimization model for charging scheduling of electric vehicles under uncertainties of vehicle availability and charging demand. J Clean Prod 2020;254:119886. http://dx.doi.org/10.1016/j.jclepro.2019.119886, URL: https://www.sciencedirect.com/science/article/pii/S0959652619347560.
[40] Weiller C. Plug-in hybrid electric vehicle impacts on hourly electricity demand in the United States. Energy Policy 2011;39:3766–78. http://dx.doi.org/10.1016/j.enpol.2011.04.005, URL: https://www.sciencedirect.com/science/article/pii/S0301421511002886.
[41] Xu Z, Hu Z, Song Y, Wang J. Risk-averse optimal bidding strategy for demand-side resource aggregators in day-ahead electricity markets under uncertainty. IEEE Trans Smart Grid 2017;8:96–105. http://dx.doi.org/10.1109/TSG.2015.2477101, URL: https://ieeexplore.ieee.org/abstract/document/7275175.
[42] Ding Z, Lu Y, Zhang L, Lee W-J, Chen D. A stochastic resource-planning scheme for PHEV charging station considering energy portfolio optimization and price-responsive demand. IEEE Trans Ind Appl 2018;54:5590–8. http://dx.doi.org/10.1109/TIA.2018.2851205, URL: https://ieeexplore.ieee.org/abstract/document/8399523.
[43] Zheng Y, Yu H, Shao Z, Jian L. Day-ahead bidding strategy for electric vehicle aggregator enabling multiple agent modes in uncertain electricity markets. Appl Energy 2020;280:115977. http://dx.doi.org/10.1016/j.apenergy.2020.115977, URL: https://www.sciencedirect.com/science/article/pii/S0306261920314276.
[44] Al-Awami AT, Sortomme E. Coordinating vehicle-to-grid services with energy trading. IEEE Trans Smart Grid 2012;3:453–62. http://dx.doi.org/10.1109/TSG.2011.2167992, URL: http://ieeexplore.ieee.org/document/6075307/.
[45] Balram P, Tuan Le A, Bertling Tjernberg L. Stochastic programming based model of an electricity retailer considering uncertainty associated with electric vehicle charging. In: 2013 10th international conference on the European energy market. 2013, p. 1–8. http://dx.doi.org/10.1109/EEM.2013.6607404, URL: https://ieeexplore.ieee.org/abstract/document/6607404.

[46] Aliasghari P, Mohammadi-Ivatloo B, Abapour M. Risk-based scheduling strategy for electric vehicle aggregator using hybrid Stochastic/IGDT approach. J Clean Prod 2020;248:119270. http://dx.doi.org/10.1016/j.jclepro.2019.119270, URL: https://www.sciencedirect.com/science/article/pii/S095965261934140X.

[47] Sánchez-Martín P, Lumbreras S, Alberdi-Alén A. Stochastic programming applied to EV charging points for energy and reserve service markets. IEEE Trans Power Syst 2016;31:198–205. http://dx.doi.org/10.1109/TPWRS.2015.2405755.

[48] Liu Z, Wu Q, Ma K, Shahidehpour M, Xue Y, Huang S. Two-stage optimal scheduling of electric vehicle charging based on transactive control. IEEE Trans Smart Grid 2019;10:2948–58. http://dx.doi.org/10.1109/TSG.2018.2815593, URL: https://ieeexplore.ieee.org/document/8315146/.

[49] Silva P, Osorio G, Gough M, Santos S, Home-Ortiz J, Shafie-khah M, et al. Two-stage optimal operation of smart homes participating in competitive electricity markets. In: 2021 IEEE international conference on environment and electrical engineering and 2021 IEEE industrial and commercial power systems europe. Bari, Italy: IEEE; 2021, p. 1–6. http://dx.doi.org/10.1109/EEEIC/ICPSEurope51590.2021.9584775, URL: https://ieeexplore.ieee.org/document/9584775/.

[50] Meese J, Schnittmann E, Schmidt R, Zdrallek M, Armoneit T. Optimized charging of electrical vehicles based on the day-ahead auction and continuous intraday market. In: 2nd e-mobility power system integration symposium. Sweden: Stockholm; 2018, URL: https://mobilityintegrationsymposium.org/wp-content/uploads/sites/10/2018/11/2C_3_Emob18_047_paper_Jan_Meese.pdf.

[51] Chemudupaty R, Ansarin M, Bahmani R, Fridgen G, Marxen H, Pavić I. Impact of minimum energy requirement on electric vehicle charging costs on spot markets. In: 2023 IEEE belgrade powertech. Belgrade, Serbia: IEEE; 2023, p. 01–6. http://dx.doi.org/10.1109/PowerTech55446.2023.10202936, URL: https://ieeexplore.ieee.org/document/10202936/.

[52] Corinaldesi C, Schwabeneder D, Lettner G, Auer H. A rolling horizon approach for real-time trading and portfolio optimization of end-user flexibilities. Sustain Energy Grid Netw 2020;24:100392. http://dx.doi.org/10.1016/j.segan.2020.100392, URL: https://www.sciencedirect.com/science/article/pii/S2352467720303234.

[53] Baule R, Naumann M. Volatility and dispersion of hourly electricity contracts on the german continuous intraday market. Energies 2021;14:7531. http://dx.doi.org/10.3390/en14227531, number: 22 Publisher: Multidisciplinary Digital Publishing Institute.

[54] Frendo O, Graf J, Gaertner N, Stuckenschmidt H. Data-driven smart charging for heterogeneous electric vehicle fleets. Energy AI 2020;1:100007. http://dx.doi.org/10.1016/j.egyai.2020.100007, URL: https://www.sciencedirect.com/science/article/pii/S2666546820300070.

[55] Wu J, Hu J, Ai X, Zhang Z, Hu H. Multi-time scale energy management of electric vehicle model-based prosumers by using virtual battery model. Appl Energy 2019;251:113312. http://dx.doi.org/10.1016/j.apenergy.2019.113312, URL: https://www.sciencedirect.com/science/article/pii/S0306261919309869.

[56] Narajewski M, Ziel F. Econometric modelling and forecasting of intraday electricity prices. J Commod Mark 2020;19:100107. http://dx.doi.org/10.1016/j.jcomm.2019.100107, URL: https://www.sciencedirect.com/science/article/pii/S2405851319300728.

[57] Nobis C, Kuhnimhof T. Mobilitaet in deutschland. Technical report, Bundesministerium für Verkehr und digitale Infrastruktur; 2018, URL: http://www.mobilitaet-in-deutschland.de/pdf/MiD2017_Ergebnisbericht.pdf, num Pages: 136.

[58] C Europe. Navigating Europe's EV Charging expansion. 2023, URL: https://statzon.com/insights/ev-charging-points-europe.

[59] Xu B, Arjmandzadeh Z. Parametric study on thermal management system for the range of full (Tesla Model S)/ compact-size (Tesla Model 3) electric vehicles. Energy Convers Manage 2023;278:116753. http://dx.doi.org/10.1016/j.enconman.2023.116753, URL: https://www.sciencedirect.com/science/article/pii/S0196890423000997.

[60] Triviño A, González-González JM, Aguado JA. Wireless power transfer technologies applied to electric vehicles: A review. Energies 2021;14:1547. http://dx.doi.org/10.3390/en14061547, URL: https://www.mdpi.com/1996-1073/14/6/1547, number: 6 Publisher: Multidisciplinary Digital Publishing Institute.

[61] Khaligh A, D'Antonio M. Global trends in high-power on-board chargers for electric vehicles. IEEE Trans Veh Technol 2019;68:3306–24. http://dx.doi.org/10.1109/TVT.2019.2897050, URL: https://ieeexplore.ieee.org/document/8633386, conference Name: IEEE Transactions on Vehicular Technology.

[62] Fama EF. Efficient capital markets: A review of theory and empirical work. J Finance 1970;25:383–417. http://dx.doi.org/10.2307/2325486, URL: https://www.jstor.org/stable/2325486, publisher: [American Finance Association, Wiley].

[63] CPE Ltd. Fee schedule. Technical report, CROATIAN POWER EXCHANGE Ltd.; 2024, URL: https://www.cropex.hr/images/6_Fee_Schedule.pdf.

[64] T GmbH. reBAP. 2024, URL: https://www.transnetbw.de/de/strommarkt/bilanzierung-und-abrechnung/rebap.

[65] HT GmbH, A GmbH, TT GmbH, T GmbH. NETZTRANSPARENZ.DE. 2024, URL: https://www.netztransparenz.de/de-de/Regelenergie/Ausgleichsenergiepreis/reBAP.

[66] ACER. ACER's final assessment of the EU wholesale electricity market design. Technical report, ACER; 2022, URL: https://www.acer.europa.eu/Publications/Final_Assessment_EU_Wholesale_Electricity_Market_Design.pdf.

[67] Varrette S, Bouvry P, Cartiaux H, Georgatos F. Management of an academic HPC cluster: the UL experience. 2014, http://dx.doi.org/10.1109/HPCSim.2014.6903792.

[68] Meeus L. The evolution of electricity markets in Europe. 2020, http://dx.doi.org/10.4337/9781789905472.